

1     **Trace metal characterization of aerosol particles and cloud**  
2                     **water during HCCT 2010**

3  
4     **Khanneh Wadinga Fomba<sup>1</sup>, Dominik van Pinxteren<sup>1</sup>, Konrad Müller<sup>1</sup>, Yoshiteru**  
5     **linuma<sup>1</sup>, Taehyoung Lee<sup>2,\*</sup>, Jeffrey L. Collett Jr.<sup>2</sup>, and Hartmut Herrmann<sup>1</sup>**

6  
7  
8     [1] Leibniz-Institute for Tropospheric Research (TROPOS), Permoserstr. 15, 04318 Leipzig,  
9         Germany

10    [2] Department of Atmospheric Science, Colorado State University, Ft. Collins, CO, 80523, USA

11    [\*] Now at: Hankuk University of Foreign Studies, Department of Environmental Sciences,  
12    Yongin, South Korea

13    Correspondence to: Hartmut Herrmann (herrmann@tropos.de)

## 1 **Abstract**

2 Trace metal characterization of bulk and size resolved aerosol and cloud water samples were  
3 performed during the Hill Cap Cloud Thuringia (HCCT) campaign. Cloud water was collected at  
4 the top of Mt. Schmücke while aerosol samples were collected at two stations upwind and  
5 downwind of Mt. Schmücke. Fourteen trace metals including Ti, V, Fe, Mn, Co, Zn, Ni, Cu, As,  
6 Sr, Rb, Pb, Cr, and Se were investigated during four full cloud events (FCE) that fulfilled the  
7 conditions of a continuous air mass flow through the three stations. Aerosol particle trace metal  
8 concentrations were found to be lower than those observed in the same region during previous  
9 field experiments but were within a similar range to those observed in other rural regions in  
10 Europe. Fe and Zn were the most abundant elements with concentration ranges of 0.2 -  
11 111.6 ng/m<sup>3</sup> and 1.1 - 32.1 ng/m<sup>3</sup>, respectively. Fe, Mn and Ti were mainly found in coarse mode  
12 aerosols while Zn, Pb and As were mostly found in the fine mode. Correlation and enrichment  
13 factor analysis of trace metals revealed that trace metals such as Ti and Rb were mostly of crustal  
14 origin while trace metals such as Zn, Pb, As, Cr, Ni, V, and Cu were of anthropogenic origin.  
15 Trace metals such as Fe, Mn, were of mixed origins including crustal and combustion sources.  
16 Trace metal cloud water concentration decreased from Ti, Mn, Cr, to Co with average  
17 concentrations of 9.18 µg/l, 5.59 µg/l, 5.54 µg/l, and 0.46 µg/l, respectively. A non-uniform  
18 distribution of soluble Fe, Cu and Mn was observed across the cloud drop sizes. Soluble Fe and  
19 Cu were found mainly in cloud droplets with diameters between 16 and 22 µm while Mn was  
20 found mostly in larger drops greater than 22 µm. Fe (III) was the main form of soluble Fe  
21 especially in the small and larger drops with concentrations ranging from 2.2 µg/l to 37.1 µg/l. In  
22 contrast to other studies, Fe (II) was observed mainly in the evening hours, implying its presence  
23 was not directly related to photochemical processes. Aerosol cloud interaction did not lead to a  
24 marked increase in soluble trace metal concentrations, but led to differences in the chemical  
25 composition of the aerosol due to preferential loss of aerosol particles through physical processes  
26 including cloud drop deposition to vegetative surfaces.

27

28

## 1 **1. Introduction**

2 Aerosol trace metals play important roles in aerosol cloud interactions as they can serve as good  
3 catalysts for aqueous phase reactions. They are useful in understanding chemical processes and in  
4 the identification of parameters that are important in controlling aerosol behavior. Dissolved trace  
5 metals can form complexes with water, sulfate, and organic compounds and can thereby  
6 influence their redox cycles (Zuo and Hoigne, 1994; Jacob and Hoffmann, 1983). They play  
7 important roles in the oxidation of S (IV) to S (VI) which has been shown to substantially  
8 influence the sulfate budget and thus the formation of cloud droplets (Harris et al., 2013).  
9 Transition metal ions such as iron and copper significantly influence the OH radical budget in  
10 aqueous media as they can react efficiently with many oxidizing and reducing agents such as  
11 HO<sub>2</sub>/O<sub>2</sub> radicals and hydrogen peroxide in aqueous media (Deguillaume et al., 2005; Spokes et  
12 al., 1994). On the other hand photochemical dissociation of metal complexes may also lead to  
13 sources of OH radicals and hydrogen peroxide. Trace metals, therefore, play important roles in  
14 the variation of the oxidative capacity of the atmosphere (Deguillaume et al., 2005; Spokes et al.,  
15 1994). Nevertheless, their reactivity is closely related to their concentrations in aqueous media  
16 (Clarke and Radojevic, 1987). To assess the importance and further understand the various  
17 reactions that are influenced by trace metals, it is necessary to quantify their concentrations in  
18 cloud drops and aerosol particles.

19 Trace metals in continental aerosols originate from extremely complex mixtures of gaseous and  
20 particulate components comprising of motor vehicle emissions, abrasion of tires or brake linings,  
21 road dust, fly ashes from wood, coal, lignite and oil combustion, refuse incineration, and also  
22 crustal weathering. This mixture influences the chemical composition and properties of the  
23 aerosol as well as the state at which trace metals are available in the aerosol particles. Depending  
24 on the location and meteorological conditions, the sources of trace metals can differ significantly,  
25 leading to variations in the trace metal and chemical composition of the aerosol. Trace metal  
26 concentrations vary according to their sources. Crustal sources are usually found to strongly  
27 influence concentrations of trace metals such as Fe, Al, Ti and Mn with concentration ranges of  
28 up to a few  $\mu\text{g}/\text{m}^3$ , especially during dust storms. However, in rural and continental background  
29 regions, trace metal concentrations are relatively lower. In cloud water a wide range of  
30 concentrations has been observed (Deguillaume et al., 2005) which has also been found to  
31 influence the chemical reactions they take part in, as well as the composition of the aerosol after

1 cloud processing. During the past years some studies have reported trace metal concentrations in  
2 different cloud conditions during various field measurements (Plessow et al., 2001; Cini et al.,  
3 2002; Hutchings et al., 2009; Mancinelli et al., 2005; Burkhard et al., 1992; Siefert et al., 1998;  
4 Liu et al., 2012; Brüggemann et al., 2005; Wang et al., 2014; Straub et al., 2012; Li et al., 2013;  
5 Guo et al., 2012; Rao and Collett, 1998) showing strong variability due to the location and air  
6 mass history.

7 During the Hill Cap Cloud Thuringia (HCCT) experiment that took place in autumn 2010, trace  
8 metals were characterized both in aerosol particles at two valley stations, upwind of and  
9 downwind from the Schmücke mountain, as well as in cloud water collected at the top of the  
10 mountain. The aim was to characterize the trace metal content in the aerosol before and after the  
11 particles interact with the cloud and also in cloud water in order to investigate the role of trace  
12 metals in altering the chemical composition of the cloud and the properties of the particles after  
13 passing through the cloud. Four full cloud events (FCE) during which the air mass was found to  
14 have traveled through all three stations and the strict criteria of the experiment were fulfilled as  
15 described in Tilgner (2014) were chosen. In this study the temporal variation of the trace metals  
16 during the selected FCE and the changes in trace metal particle size distribution and their  
17 properties after the passage of the particles through the cloud will be presented.

## 18 **2. Experimental setup**

### 19 **2.1 Sampling site**

20 The HCCT-2010 experiment was carried out in the Thüringer Wald, Germany. Based on the  
21 experience from the previous FEBUKO (Herrmann et al., 2005) field studies at the same site,  
22 sampling was done in the months of September and October in 2010. Three measurement stations  
23 were built. One in-cloud mountain station, Mt. Schmücke, and two valley stations, Goldlauter  
24 (GL, upwind of the summit station) and Gehlberg (GB, downwind of the summit station) were  
25 setup. Cloud water collection was carried out only at Mt. Schmücke while aerosol particle  
26 sampling was conducted at the valley stations. A detailed description of the experiment, sampling  
27 site and meteorological conditions during the experiment has been reported by Tilgner et al.  
28 (2014).

## 1    **2.2    Aerosol sampling**

2    Size resolved aerosol particle sampling was conducted using a humidity controlled low pressure  
3    five-stage Berner impactor with a PM<sub>10</sub> cut off. The collected particle diameter ranged from 0.05  
4    to 10 µm with lower stage cutoffs (stages 1 to 5) at aerodynamic diameters of 0.05 µm, 0.14 µm,  
5    0.42 µm, 1.2 µm and 3.5 µm, respectively. For the regulation of the humidity, seven parallel  
6    tubes were used after the isokinetic inlet to regulate the relative humidity to approx. 80 % via  
7    heating/cooling of the tubes. This was done in order to avoid water condensation on the  
8    impaction substrates under very humid conditions during cloud appearance at Mt. Schmücke and  
9    particle bounce off during very dry condition. The impactors were operated with aluminum foils  
10   and polycarbonate foils placed upon them as impaction substrates. The aluminum foils were used  
11   for aerosol mass, organic/elemental carbon (OC/EC) and inorganic ions as well as levoglucosan  
12   analysis, while the polycarbonate foils were used for trace metal analysis. Bulk particulate matter  
13   sampling was completed on Munktell quartz fiber filters using a high-volume sampler (Digital  
14   DHA-80) with a PM<sub>10</sub> inlet. The inlet height of the collectors was 4 m above ground level.

## 15   **2.3    Cloud water sampling**

16   Bulk cloud water was collected using 4 stainless steel compact Caltech Active Strand Cloudwater  
17   Collectors (CASCC2) (Demoz et al., 1996). As will be further discussed below, due to the  
18   utilization of the stainless steel collector, high blanks of some trace metals were observed. For  
19   size resolved cloud water collection, a 3-stage plastic CASCC (Raja et al., 2008) cloud water  
20   collector with nominal cloud droplet cutoffs (50% lower cut size specified as drop diameter) at 4  
21   µm, 16 µm and 22 µm was used. Bulk cloud water samples were collected every hour, while  
22   size-resolved samples were taken at a 2 h time resolution during cloud events. Aliquots were  
23   taken immediately after sample collection for on-site analysis or stabilization of trace species and  
24   the remainders of the sample volumes were frozen. For soluble trace metal redox state analysis,  
25   which was completed immediately after collection of the samples at the sampling site, 1 ml cloud  
26   water was filtered through a 0.45 µm syringe filter and 0.5 ml filtrate was obtained for the  
27   analysis.

## 28   **2.4    Chemical analysis**

29   Total trace metal analysis was performed using Total reflection X-Ray Fluorescence (TXRF)  
30   analysis. Size resolved trace metals were analyzed from the polycarbonate foils that were placed

1 on the aluminum foils on each impactor stage. Only filters from impactor stages 1 to 4 were used  
2 for trace metal analysis since impaction spots on the 5<sup>th</sup> stage were mostly not visible. Thus the  
3 trace metal concentration at the valley stations is representative of PM<sub>3.5</sub>. For TXRF analysis, the  
4 impacted spots on the polycarbonate foils were cut and placed on a TXRF carrier and were spiked  
5 with conc. HNO<sub>3</sub> and Ga (as an internal standard) and subsequently left to evaporate at 100°C.  
6 The carrier was thereafter, cooled to room temperature and measured. Blank filters that were  
7 loaded in the impactor but no air sucked through them were also analyzed using the same  
8 procedure as the sampled filters. Further details of the sample preparation procedure as well as  
9 the limitations of this method have been previously described (Fomba et al., 2013). The analyzed  
10 aerosol trace metals were Ti, V, Cr, Mn, Fe, Co, Ni, Cu, Zn, Se, Pb, As, Rb and Sr. Trace metal  
11 blank correction for the aerosol samples was performed by subtracting the elemental average  
12 concentrations of the blank filters from each analyzed sample. Due to this procedure, values for  
13 trace metals with low concentrations (< 0.01 ng/m<sup>3</sup>) especially for the fine mode particles in  
14 stages 1 and 2 were accompanied with uncertainties of about 15 % especially for metals such as  
15 V, As, and Sr. PM<sub>10</sub> soluble aerosol trace metals were also analyzed using TXRF from 0.45 µm  
16 syringe filtrates of PM<sub>10</sub> filters extracted in deionized (DI) water. The extracts were filtered in  
17 order to eliminate the contribution of particulate matter to the measured soluble concentrations.

18 For cloud water analysis, aliquots were spiked with 69% conc. HNO<sub>3</sub> solution and heated in a  
19 water bath at 60°C for 4 h. After cooling, aliquots of 100 µl were taken and brought onto the  
20 TXRF carrier surface via pipetting (4 x 25µl). Ga was then added to the sample to serve as  
21 internal standard for the TXRF measurements. These analyses could not be performed on size  
22 resolved cloud water samples due to insufficient sample volume and were thus performed only on  
23 bulk cloud water samples. For the bulk cloud water samples only Ti, V, Cr, Mn, Co, Se, Pb, As,  
24 Rb and Sr were analyzed. Fe, Ni, Cu, and Zn were excluded from the analysis due to  
25 contamination arising from sample collection and preparation. For the analysis of  
26 organic/elemental carbon (OC/EC), inorganic ions and levoglucosan, the same procedure as  
27 described earlier (Muller et al., 2010; Iinuma et al., 2007) was used.

28 Cloud water trace metal blanks were measured from blank samples that were collected after  
29 cleaning of the stainless steel bulk cloud water collector with deionized water after each cloud  
30 event. The blanks were not subtracted since they were considered to be influenced by residual  
31 materials in the collectors from previous cloud events that were not fully removed during the

1 cleaning process. Therefore, the first collected sample of each event was not considered in the  
2 data analysis due to likely strong influence of the wash-off of the collectors. However, most trace  
3 metal blanks were lower than 25% of the hourly cloud water concentrations except for Fe, Cu, Ni  
4 and Zn whose blanks were mostly higher (up to 65%) of the hourly concentrations. The results of  
5 these 4 trace metals were thus considered to be very inaccurate and were, therefore, not  
6 considered in the further analysis of the results.

7 For the analyses of the soluble transition metal ions (TMI) redox states, a DIONEX ICS 900 ion  
8 chromatography instrument, equipped with a CS5A column and a UV-VIS detector was used.  
9 Using this instrument, transition metal ions such as Fe (III), Fe (II), Cu (II), and Mn (II) can be  
10 determined via post column derivatization simultaneously. This is performed via a procedure  
11 similar to the one reported by Oktavia et al. (2008), however using a 4-(2-pyridylazo) resorcinol  
12 (PAR, P/N 039672) as post column reagent. This combination renders a good separation of the  
13 above mentioned ions making the analysis easier to handle. TMI redox state measurements were  
14 only performed on size resolved cloud water samples. As indicated above, similar redox state  
15 measurements on bulk cloud water samples were not considered for the data interpretation due to  
16 their high blank values.

17

### 18 **3. Results and discussion**

19 The presented results are focused on data obtained during four full cloud events (FCE); FCE1.1  
20 (14/9/2010 11:00 to 15/9/2010 01:00), FCE 11.3 (02/10/10 14:30 to 19:30) , FCE 13.3  
21 (10/6/2010 12:15 to 10/7/2010 3:15), and FCE 22.1 (10/19/2010 21:30 to 10/20/2010 3:30). The  
22 results will be presented in two sections. The first section will be focused on the aerosol particle  
23 analysis and the second on the cloud water analysis.

#### 24 **3.1 Aerosol trace metal concentrations**

25 The aerosol trace metal concentrations during HCCT-2010 at the valley stations are presented in  
26 Table 1. Reported trace metal concentrations in other rural regions in Europe and during previous  
27 experiments in this region reported by Rüd (2003) are also presented in Table 1 for comparison.  
28 Amongst the 14 investigated elements, Fe was the most abundant element. Similar findings were  
29 obtained by Rüd (2003) during the FEBUKO experiment. The next most abundant trace metals

1 were Zn, Cr, and Pb. Iron concentrations were within the range of 0.2 - 111.6 ng/m<sup>3</sup> with an  
2 average value of 16.5 ng/m<sup>3</sup> while Zn, Cr, and Pb values were within the ranges of 1.1 -  
3 32.1 ng/m<sup>3</sup>, 0.4 - 21.9 ng/m<sup>3</sup> and 0.3 - 2.9 ng/m<sup>3</sup> with average values of 11.1 ng/m<sup>3</sup>, 2.7 ng/m<sup>3</sup> and  
4 1.3 ng/m<sup>3</sup>, respectively. The average aerosol particle mass concentrations of the other elements  
5 were all less than 1 ng/m<sup>3</sup> but their concentrations ranged between 0.01 ng/m<sup>3</sup> and 4 ng/m<sup>3</sup>. The  
6 concentration ranges of elements such as Cr, Mn, and Zn were within the same order of  
7 magnitude as those reported by Rüd (2003) during the FEBUKO campaign in the same location.  
8 Comparatively, the mean concentrations and the obtained concentration ranges during HCCT-  
9 2010 were in good agreement with those reported at other rural regions in Europe. For trace  
10 metals such as Cr and Zn, their mean concentrations were higher than those reported at  
11 Boccadifalco, Italy (Dongarra et al., 2010), Puy de Dôme, France (Vlastelic et al., 2014) K-  
12 Puska, Hungary (Maenhaut et al., 2008), Monte Cimone, Italy (Marenco et al., 2006) Monte  
13 Martono, Italy (Moroni et al., 2015) and at Auchencorth (UK) (Allen et al., 2001) although in the  
14 case of Zn the average concentration was comparable with that observed at Castlemorton (UK)  
15 (Allen et al., 2001) but lower than that reported at the, Schmücke (Rüd, 2003) and at Bertiz,  
16 Spain (Aldabe et al., 2011). However, the concentration ranges were similar to those reported by  
17 Rüd (2003). Trace metals such as Sr and As showed comparable average values and ranges to  
18 those reported at other rural sites in Italy (Dongarra et al., 2010; Allen et al., 2001; Hueglin et al.,  
19 2005), UK and Switzerland as well as at Bertiz (Aldabe et al., 2011) and Diabla Gora, Poland  
20 (Rogula-Kozłowska et al., 2014).

21 Se, Rb, mean concentrations were lower than those reported at Bertiz, Spain (Aldabe et al., 2011)  
22 and Puy de Dôme, France (Vlastelic et al., 2014). For trace metals such as Ti, Co, Fe, Ni, Cu, Pb,  
23 the mean concentrations were lower than those reported in the above stated sites except for Fe  
24 and Cu which were higher than the values reported at Bertiz, Spain (Aldabe et al., 2011) and at  
25 Hyytiälä, Finland (Maenhaut et al., 2011), respectively. However, the concentration ranges of  
26 these metals were within the same order of magnitude as those reported at the other rural sites.  
27 The lower average values obtained during HCCT-2010 than those reported at other rural sites are  
28 likely due to the different geographical settings of the sampling sites and the different particulate  
29 matter size ranges sampled at some of these sites. The measurements at the UK sites were based  
30 on total suspended particulate matter (TSP) while the measurements at Payerne in Switzerland  
31 (Hueglin et al., 2005) and the measurements from Rüd (2003), Puy de Dôme (Vlastelic et al.,



1 2014), (Vlastelic et al., 2014) K-Puska (Maenhaut et al., 2008) were done on PM<sub>10</sub> particles and  
2 those during HCCT-2010 on PM<sub>3,5</sub> particles. In addition, Goldlauter and Gehlberg do not  
3 experience frequent strong air mass outflow from major urban cities as do the other investigated  
4 sites. The differences in the observed concentrations between HCCT-2010 and those reported by  
5 Rüd (2003) during the FEBUKO experiment could also be due to a reduction in particulate matter  
6 emission in Germany and central Europe during the past 15 years. It has been observed in other  
7 rural regions in Germany that the PM<sub>10</sub> concentration has dropped by more than 10% within the  
8 past decade (Spindler et al., 2013). Although these values varied during the campaign as shown in  
9 their ranges, their size distributions were different as the air mass parcel crossed the mountain  
10 station to the downwind station.

11 *Please insert Table 1 here*

12

### 13 **3.1.1 Aerosol trace metal size distribution**

14 Figure 1 shows the size distribution of the trace metals during four full cloud events (FCE 1.1,  
15 FCE 11.3, FCE 13.3 and FCE 22.1). In principle, the aerosol mass may decrease during the  
16 passage of the air mass parcel through the cloud and over the mountain due to particle and/or  
17 cloud droplet deposition during air mass transit across the forested mountain. Entrainment of  
18 cleaner air from above might also reduce concentrations, or in the case of more polluted air mass  
19 from above, increases the concentration. However, during HCCT, the meteorological analysis as  
20 reported by Tilgner et al. (2014) did not show strong entrainment from more polluted air masses  
21 especially during the selected events. In Figure 1, such a trend is observed for FCE 1.1, 13.3 and  
22 22.1 wherein the total trace metal mass decreased from the upwind side (GL) to the downwind  
23 side (GB) of the mountain. During FCE 11.3, there was no significant difference in the total  
24 particle trace metal mass, suggesting there may have been limited deposition or an influence from  
25 local sources such as traffic as seen in the increase in the Cr, Cu and Ni concentrations. During  
26 FCE 1.1 Fe was mostly found in the coarse mode while Zn and Pb were mostly found in the fine  
27 modes (stages 2 and 1) at Goldlauter. In Gehlberg, the trace metal size distribution changed with  
28 the trace metals concentrated in the fine mode as compared to the coarse mode observed in  
29 Goldlauter. The different concentrations and size distributions are indicative of preferential  
30 particle loss during this event as a significant part of the concentration difference is largely due to

1 the decrease in the Fe concentration by a factor of 4 in the fourth stage. The decrease in the mass  
2 concentration is related to loss of Fe-containing material after passage of the air mass through the  
3 cloud, especially as iron is mostly found in the coarse mode. Coarse mode particles are usually  
4 emitted from mechanical processes such as re-suspension of soil particles in the atmosphere or  
5 abrasion of car parts due to friction or from other industrial processes. These particles are larger  
6 and heavier and can therefore be easily lost through deposition.

7 *Please insert Figure 1 here*

8  
9 During FCE 11.3 the size distribution did not vary largely. Although a decrease in the fine mode  
10 fraction was apparent especially due to loss of Zn and Pb containing particles, the changes in the  
11 coarse mode fraction were not significant. Cr, Cu, and Ni concentrations were found to be higher  
12 at GB. Although, entrainment of more polluted air masses may lead to an increase in the  
13 concentration of trace metals in the downwind site, meteorological studies by Tilgner et al. 2014  
14 revealed a more stable stratification during this event with no large differences observed in the  
15 coefficient of divergence of the particles, suggesting that the possibility of entrainment of  
16 polluted air masses from above was rather low. These increased trace metals are often found from  
17 traffic emissions relating to car brake wear (Maenhaut et al., 2005) or from fuel combustion (Lee  
18 and Vonlehmd.Dj, 1973). The GB measurement site was close to the main road linking GB and  
19 Mt. Schmücke and could be influenced by traffic especially during weekends (period of this  
20 event) when more touristic activities are present in this region, thus, suggesting that traffic  
21 emissions may have influenced these concentrations. A different trend was observed during the  
22 FCE 13.3 during which the total mass of the trace metals decreased. No significant changes in the  
23 shape of the size distribution of most elements were observed. The major elements observed were  
24 also Fe, Zn and Pb. A similar trend was observed during FCE 22.1 with the trace metal  
25 concentration decreasing from GL to GB and the size distribution of these metals not changing  
26 significantly. Slight increases in Cr and Cu were observed in the coarse mode fraction at GB.

27 During most of the FCE's the total trace metal concentration dropped from GL to GB preserving  
28 the size distribution. An exception was observed during FCE 11.3 where a significant difference  
29 was not observed in the coarse mode fraction. Fe, Rb, Sr, Mn and Ti were mostly found in the  
30 coarse mode while Pb, Zn, As, Se, Cr, Ni were mostly found in the fine mode aerosol particles.

1 Fe and Zn were the most deposited trace metals especially during FCE 1.1 and FCE 11.3.  
2 Although back trajectory analysis showed slight differences between the air mass origins during  
3 FCE 1.1, 11.3, and 13.3, this difference was not strongly reflected in the trace metal distributions  
4 and no significant difference in the relative contribution of a particular metal was observed.  
5 Details on the likely sources of these trace metals will be further discussed in section 3.3 below.

## 6 **3.2 Correlation between trace metals and other aerosol chemical components**

### 7 **3.2.1 Levoglucosan**

8 Figure 2 shows scatter plots of levoglucosan with potassium, zinc, lead and arsenic in the  
9 particulate matter at the upwind (GL) and downwind (GB) stations in  $PM_{1.2}$  particles. These  
10 elements showed good correlation with levoglucosan, both in  $PM_{1.2}$  and  $PM_{3.5}$  particles. The p-  
11 values of these plots were less than 0.05. Nevertheless, since these correlations are based on  
12 statistically few data points their values are used to mainly indicate possible trends between these  
13 components. In some cases these trends match observations observed elsewhere. Alongside  
14 potassium, levoglucosan is known (Schkolnik and Rudich, 2006; Simoneit et al., 1999; Iinuma et  
15 al., 2007) to be a good tracer for particles originating from biomass burning. The correlations  
16 with levoglucosan could be indicative of a common source, such as biomass burning. Zn  
17 amongst other elements has been observed in biomass combustion emissions (Fine et al., 2004)  
18 and although it is not largely accumulated in plants as has been observed by Schmidl et al.(2008),  
19 plumes of biomass burning as well as the applied fuel (Boman et al., 2006) or emissions from the  
20 walls of the combustion chambers can influence their concentrations in the atmosphere. These  
21 correlations, however, may also be simply due to changes in similar meteorological conditions.

22 *Please insert Figure 2 here*

23 Table 2 shows the correlation coefficients of levoglucosan and other trace metals in  $PM_{1.2}$   
24 particles at both valley stations before and after the passage of air mass through the cloud.  
25 Positive correlations were also observed for Mn and Fe with levoglucosan at Goldlauter the  
26 upwind side. However, changes in the correlations were observed as the air mass passed through  
27 the cloud at the mountain station before arriving at Gehlberg. As shown in Table 2, the  
28 correlations of K, Fe, and As with levoglucosan became weaker suggesting that deposition of  
29 levoglucosan and particles containing such metals during the air mass transport over the  
30 mountain to GB may have significantly affected the state at which these components were present

1 at GL. Levoglucosan is a water soluble compound that can dissolve in cloud water and may also  
2 be lost from particles, aqueous reaction in cloud drops, or deposition of the cloud droplets. Such  
3 losses may account for the lower (about 40%) concentration of levoglucosan observed at the  
4 downwind stations as depicted in Figure 2b and the observed change in the correlation with the  
5 trace metals observed in Table 2. Similarly, trace metals can also be deposited during their  
6 transport.

7 *Please insert Table 2 here*

8  
9 The combination of these losses may lead to differences in the correlations observed between the  
10 upwind and downwind stations. In principle, no differences in this tendency were observed for  
11 the coarse and fine mode concentrations of these components, indicating that the fine mode  
12 aerosols carried most of the observed levoglucosan. Similar observation has been reported  
13 elsewhere (Herckes et al., 2006).

### 14 **3.2.2 Elemental and organic carbon**

15 Elemental carbon (EC) is often considered as soot particles that are emitted from diesel engines,  
16 or from other combustion processes as well as from industrial emissions while organic carbon  
17 (OC) has both anthropogenic and biogenic sources (Herrmann et al., 2006; Saarikoski et al.,  
18 2008). In rural areas such as Goldlauter (GL) and Gehlberg (GB), EC could originate from  
19 combustion processes or long range transport from industrial and urban regions. Figures 3 and 4  
20 shows scatter plots of Ti, Mn, and Fe against OC as well as Pb, As, and Zn against EC at the  
21 upwind stations, respectively. The scatter plots reveal good correlation between these  
22 components in PM<sub>3,5</sub> particles. Good correlations were also observed for selenium with EC as  
23 well as Zn with OC. As explained above changes in meteorological conditions may lead to  
24 correlations between aerosol components. However, it has been observed elsewhere that these  
25 components could originate from sources such as fossil fuel or coal combustion (Hashimoto et  
26 al., 1970; Pacyna, 1984; Zhang et al., 2014), long range transport or traffic emissions relating to  
27 tire or brake wear (Handler et al., 2008).

28 *Please insert Figures 3 and 4 here*

1  
2 EC correlation with Pb, Se, As and Zn remained stable after passage of air masses through the  
3 cloud, implying that the Se, Pb or As containing material might have not been strongly deposited  
4 or lost during their transport through the cloud or the deposition of these metals and EC were  
5 similar. Apparently, these elements are mostly present in particles in the fine mode. OC also  
6 showed good correlation with Fe after passage of air mass through the cloud but poor correlation  
7 with Ti and Mn. The poor correlation after passage of air mass through the cloud as already  
8 explained above is probably related to preferential loss via wet or dry deposition of Ti or Mn as  
9 well as of OC/EC containing particles.

### 10 **3.2.3 Other correlations**

11 At the upwind station, oxalate showed good correlation with iron ( $r^2 = 0.69$ ). This correlation  
12 between oxalate and iron as also observed above for iron and organic carbon indicates that the  
13 studied aerosols could be aged aerosols from sources such as biomass burning or even crustal  
14 sources especially for the coarse mode fractions. This correlation did not change significantly  
15 after the passage of the air parcel through the cloud especially during the FCEs. Despite the fact  
16 that the photolysis of iron oxalate complexes in aqueous media is known (Weller et al., 2013) to  
17 lead to the destruction of oxalate which may indirectly lead to a poor correlation between iron  
18 and oxalate after the air mass passes through the cloud, and also particulate matter loss due to  
19 droplet deposition, a significant change of the correlation was not observed. However, this could  
20 also be due to the fact that most of the cloud events were observed in the evening hours where  
21 photochemical processes such as photolysis are not significant.

22

### 23 **3.3 Enrichment factor analysis**

24 Enrichment factor (EF) analysis was performed on  $PM_{3.5}$  aerosol trace metals to evaluate the  
25 contribution of crustal material to the aerosol trace metals obtained at the valley stations. The  
26 evaluation was done using (Wedepohl, 1995) upper continental crust composition with Ti chosen  
27 as a marker for crustal material. The EF of an element Z in the aerosol with respect to its  
28 composition in the crust is given as

$$EF = \frac{(Z/Ti)_{Aerosol}}{(Z/Ti)_{Crust}}$$

29 An enrichment factor above 10 is considered as a significant enrichment of the element and

1 below 0.70 as a strong depletion in comparison to the composition of the reference source.  
2 Enrichment factors between 0.70 and 2 are considered to be similar and within the error range of  
3 the reference source, implying that the elements with such factors might have originated from a  
4 similar source while enrichment factors between 2 and 10 are considered to be moderately  
5 enriched. Figure 5 shows the size resolved enrichment factors with respect to Ti for the measured  
6 elements of the various impactor stages at the valley stations GL and GB during HCCT 2010.  
7 The values are average enrichment factor values for the FCE's and the standard deviation plotted  
8 as error bars to indicate the variability of the values for each element at the various stations. As  
9 shown in Figure 5, the enrichment factors decreased with particle size with lower enrichment  
10 observed for the coarse mode fraction (such as stage 4) in comparison to the fine mode fraction  
11 (stages 1 and 2). In principle, no significant difference especially for the fine mode particles was  
12 observed between the enrichment factors of the elements at the upwind and downwind stations,  
13 implying that the aerosol cloud interactions did not lead to heavy loss of only a particular element  
14 with respect to Ti. Slight differences were observed with slightly higher enrichment factors  
15 observed at the downwind stations in comparison to the upwind station in the coarse mode  
16 fraction. This slight increase could be as a result of preferential loss through, for example,  
17 deposition processes of crustal material containing Ti which is more present in the coarse mode  
18 than in the fine mode.

19 *Please insert Figure 5 here*

20

21 Despite these changes, clear trends with increasing enrichment factors from Rb to Se could be  
22 observed. Trace metals were identified and grouped according to their similar EF. One group of  
23 trace metals including Mn, Fe, Co, Rb and Sr showed little to no enrichment at all the stages at  
24 both the upwind and downwind stations with  $EF < 10$  indicating that their occurrences were  
25 predominantly of crustal origin. Slightly elevated enrichment factors observed for Fe and Mn in  
26 fine mode fraction stages 2 and 3 is likely related to the emission of these elements from other  
27 sources such as coal combustion as well as biomass burning. The good correlations observed  
28 above between iron and oxalate or levoglucosan as well as between Mn, Fe, and organic carbon is  
29 a further indication of the likely influence of these combustion sources. The second group of  
30 elements includes V, Cr and Ni. These elements showed high enrichment at all the stages and at

1 both stations indicating they were of anthropogenic origin. Such metals are known to originate  
2 from fuel oil or coal combustion (Lee and Vonlehmd.Dj, 1973). The last group of trace metals  
3 including Cu, Zn, AS, Pb and Se, showed very high enrichment factors with values higher than  
4 1000 in the fine mode. The very high enrichment is also indicative of their anthropogenic origins.  
5 Cu and Zn are known to be emitted from exhaust gas (Pakkanen et al., 2003) and also car brake  
6 linings and tire wear in urban aerosols (Maenhaut et al., 2005). Zn, As, Se, and Pb have been  
7 observed from high temperature combustion processes such as coal combustion or waste  
8 incineration processes as well as from non-metallurgic industrial processes (Belis et al., 2013;  
9 Minguillon et al., 2007; Pacyna et al., 2007). The correlations observed between Zn, As, Pb, and  
10 elemental carbon further supports the likely influence of such sources. These metals were also  
11 strongly enriched in the fine fraction of the aerosol particles and could have also originated from  
12 long range transport due to the long atmospheric lifetimes of fine particles. Back trajectory  
13 analysis of the air masses during these four events showed that the air masses crossed populated  
14 and industrial regions in Germany and France prior to their arrival at the measurement site.

15

### 16 **3.4 Cloud water trace metal concentration**

17 The average concentrations and the range of the various metal concentrations observed at Mt.  
18 Schmücke are presented in Table 3. Reported concentrations from previous FEBUKO experiment  
19 performed at the same location in 2002 and also reported concentrations from fog and cloud  
20 measurements done at other mountain sites in the world are also presented. For comparison of the  
21 cloud data with the valley stations, and for the understanding of the changes from sample to  
22 sample, and to obtain the equivalent air loading, the variation of the liquid water content (LWC),  
23 which alters dilution of solutes in the cloud water, was removed by multiplying the cloud water  
24 aqueous concentration with the LWC.

25 *Please insert Table 3 here*

26

27 Trace metal concentrations decreased from Ti, Mn, Cr, to Co in cloud water. The average Ti  
28 concentration was observed at 9.8  $\mu\text{g/l}$  ( $2.6 \text{ ng/m}^3$ ) while for Mn, Cr and Co, average  
29 concentrations of 5.59  $\mu\text{g/l}$  ( $1.54 \text{ ng/m}^3$ ), 5.54  $\mu\text{g/l}$  ( $1.5 \text{ ng/m}^3$ ) and 0.46  $\mu\text{g/l}$  ( $0.13 \text{ ng/m}^3$ ),

1 respectively, were observed. The average concentrations of Sr, Pb, and Se ranged between  
2 1.38 µg/l to 2.45 µg/l while for V, As, Rb, and Co, their concentrations were < 1 µg/l. Compared  
3 to previous FEBUKO experiments, apart from Cr, the average trace metal concentrations  
4 observed during HCCT were lower for most of the elements but their concentration ranges were  
5 similar to those observed during FEBUKO. The lower average concentrations might be due to  
6 reduction in particulate matter emissions over the time period of these studies in this area. Pb  
7 concentrations during HCCT were lower than those reported at Mt. Brocken (Plessow et al.,  
8 2001) and at Fichtelgebirge (Wrzesinsky and Klemm, 2000) but were higher than those reported  
9 in fogs at rural regions in Pennsylvania (Straub et al., 2012) and in marine clouds (Vong et al.,  
10 1997; Wang et al., 2014). Rb, Sr and As concentrations were similar to those observed at Mt.  
11 Brocken. However, As values were lower than those observed at Fichtelgebirge (Wrzesinsky and  
12 Klemm, 2000). Mn and Se concentrations were within a similar order of magnitude as those  
13 reported at Mt. Brocken, Fichtelgebirge and in marine clouds. However, the concentrations were  
14 far lower than those reported in cloud water at Mt. Tai, china (Guo et al., 2012; Liu et al., 2012).  
15 Lower concentrations than those observed in this study have also been reported by Wang et al.  
16 (2014) at higher elevated stratocumulus clouds collected via measurements using aircraft in  
17 California. The differences in these concentrations are related to differences in location and  
18 source influence, hence differences in air mass origin and in the cloud droplet composition.

19

### 20 **3.4.1 Temporal variation of trace metals during selected FCE**

21 Figure 6 shows the temporal variation of the trace metals during the four FCE and the variations  
22 between the cloud events. Often, higher trace metal concentrations were observed during the first  
23 hours of the events and subsequently decreased during the course of the event. This trend was  
24 mostly observed during FCE 1.1 and FCE 11.3 while during FCE 1.1 very small differences were  
25 observed between the temporal variations of the metals. During FCE 1.1 the trace metal  
26 concentrations show uniform variation with slight increase in concentrations observed after 17:00  
27 h. While As, Pb, Se, V, and Mn, showed similar trends, Ti and Cr showed very different patterns.  
28 Similar trends were observed during FCE 11.3, 13.3 and FCE 22.1 for As, Pb and Mn. Ti trends  
29 were unique throughout the FCE. During FCE 13.3 and FCE 22.1, Co, V, Cr, showed similar  
30 temporal variations. The temporal variations in the trace metal concentrations are likely due to



1 the temporal changes in the trace metal concentrations in the activated cloud condensation nuclei  
2 (CCN) and changes in air mass origin. The similar trend in the temporal variation of the trace  
3 metals is indicative of their similar origin. Ti is a good tracer for crustal sources while Pb and V  
4 are good tracers of anthropogenic activities. Thus the origins of the trace metals were similar  
5 throughout most of the events and were of anthropogenic and crustal origins.

6 *Please insert Figure 6 here*

7

### 8 **3.4.2 Size resolved soluble metal ions**

9 Soluble Fe (III), Fe (II), Cu (II) and Mn (II) were measured from 0.45  $\mu\text{m}$  syringe filtered  
10 samples collected using a plastic 3-stage CASCC collector with Teflon collection surfaces.  
11 However, because of low sampling amounts only the analyses during FCE 1.1 were successful.  
12 The size distribution and temporal variations of these ions are shown in Fig. 7 . The nominal  
13 cloud water size cut-offs were 22  $\mu\text{m}$ , 16  $\mu\text{m}$  and 4  $\mu\text{m}$  for stages (St.) 1, 2 and 3, respectively. Fe  
14 (II) was mainly found on the second stage (size range: 16 - 22  $\mu\text{m}$ ) with concentrations of up to  
15 28.2  $\mu\text{g/l}$  meanwhile Fe (III) was found on all of the stages during the event with observed  
16 concentrations ranging up to 37.1  $\mu\text{g/l}$ . The lowest concentration of Fe (III) was found in the  
17 larger droplets (stage 1). Soluble Cu (II) was concentrated in the first and second stages, likewise  
18 Mn (II). The Cu (II) concentrations ranged from 0.4  $\mu\text{g/l}$  to 10.5  $\mu\text{g/l}$  with higher concentrations  
19 observed on the second stage. Mn (II) concentrations varied from 1.1  $\mu\text{g/l}$  to 24.5  $\mu\text{g/l}$  with about  
20 48% present in the larger droplets (stage 1) which was different to the size distribution of the  
21 other measured transition metal ions (TMIs).

22 Similar soluble trace metal concentrations have been reported in fogs (Straub et al., 2012) and  
23 cloud water (Li et al., 2013; Parazols et al., 2006; Hutchings et al., 2009) in other regions. The  
24 differences in the size distribution of these trace metals suggest that these TMIs might have had  
25 different source origins especially for Mn and Fe. Although Mn as well as Fe has high crustal  
26 abundance, both also have different anthropogenic sources such as waste incineration or  
27 metallurgical industries for Mn and fly ash for Fe. Fine mode iron can also be emitted from fuel  
28 combustion processes (Sholkovitz et al., 2012) which can thus explain its occurrence in this size  
29 fraction. Thus the differences in the size distribution of these metal ions could be due to their  
30 source origins during this event or the differences in the efficiency of activation of the particles

1 containing these metals. Fe (II) was observed mostly during evening hours during which  
2 photochemical processes are expected to be low due to lower solar radiation. This indicates that  
3 the observed night time Fe (II) concentrations were not directly related to photochemical  
4 processes. Fe (III) is known to be the most stable form of iron but it can be reduced to Fe (II) via  
5 HO<sub>x</sub> radicals or Cu (I). The production of HO<sub>x</sub> radicals is predominantly photochemically driven.  
6 Their reactions with Fe(III) are, therefore expected to be faster in the present of UV light such as  
7 during daytime; meanwhile, the reduction of Fe (III) to Fe (II) via Cu (I) is not directly limited by  
8 solar radiation and thus could be dominant at night (Deguillaume et al., 2004).

9 *Please insert Figure 7 here*

10 Due to the fast oxidation of Cu (I) to Cu (II) it is easier to measure Cu (II) than Cu (I). During  
11 FCE 1.1 Cu (II) was successfully measured with results revealing comparable concentrations as  
12 those reported elsewhere (Deguillaume et al., 2005; Li et al., 2013; Hutchings et al., 2009). The  
13 Cu (II) temporal variation is also shown in Figure 7. The observed Cu (II) concentration in the  
14 same size fraction as soluble iron indicates that the Fe (II) at night could have been related to  
15 aqueous phase reductions of Fe (III) to Fe (II) by Cu (I) species. Fe (III) catalyzed oxidation of  
16 sulfur (IV) has been suggested to be another important source of Fe (II) in cloud water during  
17 nighttime (Schwanz, 1998; Millero et al., 1995). However, with no data available on sulfur (IV)  
18 measurements during FCE1.1, conclusions about the contribution of this pathway cannot be  
19 made. Anthropogenic sources of Fe in the environment, e.g. in fly ash, biomass burning  
20 emissions and other combustion sources have been found to contain considerable concentration  
21 of Fe (II) (Trapp et al., 2010). This suggests that, although aqueous phase reduction processes  
22 could have contributed to the observed night time Fe (II) concentrations, the source of the aerosol  
23 cannot be neglected. Night time concentrations of Fe (II) have also been observed in different  
24 studies but no unique reason for their occurrence has been presented yet (Schwanz, 1998;  
25 Kotronarou and Sigg, 1993; Siefert et al., 1998; Parazols et al., 2006). The variation of the  
26 soluble trace metal concentrations with cloud drop size suggests that the metal catalyzed  
27 oxidation of S (IV) may be strongly drop size dependent since the concentrations of TMI  
28 influence the in cloud S (IV) oxidation rates (Rao and Collett, 1998).

## 1 **3.5 Comparison between trace metal concentrations in cloud water and in** 2 **particles**

### 3 **3.5.1 Total trace metal concentration**

4 As shown in Tables 1 and 3, Mn, Rb and Ti in cloud water were higher than at the valley stations.  
5 However, although the average values for Mn and Ti were higher in cloud water as compared to  
6 those from the valley stations, the concentration ranges were similar. One reason for the  
7 observed difference in the Mn, Ti and Rb concentrations could have been the analyzed particle  
8 size from the impactor samples collected from the valley stations. Mn, Ti and Rb are often of  
9 crustal origin and also often found in the coarse aerosol fraction. As explained above, the aerosol  
10 trace metal analysis was performed only on PM<sub>3.5</sub> particles. Thus the difference in the sampled  
11 particle sizes may explain the observed difference. For other trace metals such as V, Co, Se, As  
12 and Sr, only small differences were observed with slightly lower concentrations observed in the  
13 cloud water in comparison to those at the valley stations. The average Pb and Cr, concentrations  
14 were also lower in cloud water as compared to the concentrations at the valley stations. The  
15 observed differences between the cloud water and aerosol particle concentrations are also related  
16 to the strong variation of the trace metal concentrations during the FCEs due to their varying  
17 sources as well as the variation in the activation of the particles to suitable cloud condensation  
18 nuclei.

### 19 **3.5.2 Soluble trace metal concentration**

20 Soluble aerosol trace metal concentrations were measured from 0.45 µm syringe filtrates obtained  
21 from DI water extracts of PM<sub>10</sub> bulk samples and the concentrations were compared with those  
22 obtained from filtered cloud water to find out if there were significant changes in the soluble trace  
23 metal concentration after the passage of the air mass through the cloud. Table 4 summarizes the  
24 soluble metal concentrations during selected FCEs. Due to the observed high blanks of Fe, Zn,  
25 Cu, Mn in bulk cloud water samples, their values were not discussed except during FCE 1.1  
26 whereby the values of the sized resolved analysis presented above are included (in bold). The size  
27 resolved data were converted to bulk concentrations by multiplying the volume weighted mean  
28 size-resolved concentrations with the bulk LWC. As shown in Table 4, during FCE 1.1 no  
29 significant change in the soluble content of the trace metals was observed before and after the  
30 cloud. Mn, Cu, Ni, and Zn, as well as As, Se, Sr, V, Cr concentrations were of the same order of  
31 magnitude while only slight increases were registered for Pb concentrations. Cu, Mn, and Fe

1 concentrations were within same order of magnitude as those at the valley stations, suggesting  
2 that there might have been no significant in-cloud processing of the particles containing these  
3 metals that affected trace metal solubility. During FCE 11.3 small increases in the soluble  
4 concentration of Cr, Mn, Ni, Cu, Zn, As and Pb were observed between Goldlauter and Gehlberg.  
5 However, during FCE 13.3 the soluble content decreased from Goldlauter to Gelberg for  
6 elements such as V, Mn, Fe, Ni, Cu, Zn, As, Se, Rb, Sr while a slight increase could only be  
7 observed for Ti and Cr. Similarly, during FCE 22.1 an increase in soluble content was observed  
8 for Ti, V, Fe, Cu, while a decrease was observed for Cr, Mn, Ni, Zn, As, Se, Rb, Sr, and Pb.

9 *Please insert Table 4 here*

10  
11 Although it is known that cloud processes enhance the solubility of trace metals, especially for  
12 elements such as Fe via acid dissolution or complexation with organic acids such as oxalic acid,  
13 no clear trend and significant difference was observed between the upwind station (GL) and the  
14 downwind station (GB) soluble iron concentrations. Since most of the FCE were observed in the  
15 evening period, the possibilities for photochemical processes to occur were limited. As with iron,  
16 no clear trend in the variation of the soluble trace metal concentrations was observed for the other  
17 metal ions during all the FCE. The variation in the observed concentrations during the different  
18 FCE is also related to influences in air mass origin and the loss due to preferential deposition of  
19 larger or more efficiently cloud-scavenged particles.

#### 20 **4. Summary**

21 The characterization of trace metals in size resolved and bulk aerosol particles at the valley  
22 upwind (Goldlauter, GL) and downwind (Gehlberg, GB) stations as well as in cloud water at Mt.  
23 Schmücke during four cloud events during HCCT has been presented. The concentrations of the  
24 14 investigated trace metals showed variations between the cloud events with Fe and Zn being  
25 the most abundant observed trace metals in the aerosol. The most deposited trace metals between  
26 the upwind and downwind stations were also Fe and Zn. Aerosol particle trace metal  
27 concentrations were lower than those observed in the same region during the FEBUKO field  
28 experiments about 9 years ago. The decrease in metal concentrations could be related to  
29 decreases in emission as well as differences in the PM size fraction analyzed (PM<sub>3,5</sub> vs. PM<sub>10</sub>).  
30 Aerosol and cloud trace metal concentrations observed in this study were within a similar range

1 to those observed in other rural regions in Europe. Strong changes in aerosol particle chemical  
2 properties were observed as particles passed through clouds with changes in the correlation  
3 between some chemical components observed. Trace metals such as Zn, Pb, Fe, Mn and Ti  
4 showed good correlation with levoglucosan, oxalate, and organic and elementary carbon  
5 suggesting their similar source origins. In addition to correlation analysis, enrichment factor  
6 analysis showed that trace metals during HCCT were of various origins, including crustal,  
7 biomass burning, coal combustion, long range transport, and traffic sources. Soluble aerosol trace  
8 metal concentrations did not show strong variations after aerosol cloud interaction. However, size  
9 resolved soluble trace metal concentrations in cloud water showed a non-uniform distribution of  
10 Fe, Cu and Mn across the drop sizes with Cu and Fe mainly found in drop sizes between 16 and  
11 22  $\mu\text{m}$  and Mn in drop sizes greater than 22  $\mu\text{m}$ . Such variations suggest that TMI catalytic  
12 process such as TMI enhanced oxidation of S (IV) may be drop size dependent. Soluble iron was  
13 mainly found in its Fe (III) state. Strong temporal variation was observed in the soluble Fe  
14 concentrations with Fe (II) dominating the soluble iron concentrations during some episodes. In  
15 contrast to other studies, Fe (II) was mostly observed in the evening hours implying its presence  
16 in cloud water was not directly related to photochemical processes.

## 1 **References**

- 2 Aldabe, J., Elustondo, D., Santamaria, C., Lasheras, E., Pandolfi, M., Alastuey, A., Querol, X.,  
3 and Santamaria, J. M.: Chemical characterisation and source apportionment of PM<sub>2.5</sub> and  
4 PM<sub>10</sub> at rural, urban and traffic sites in Navarra (North of Spain), *Atmos Res*, 102, 191-  
5 205, DOI 10.1016/j.atmosres.2011.07.003, 2011.
- 6 Allen, A. G., Nemitz, E., Shi, J. P., Harrison, R. M., and Greenwood, J. C.: Size distributions of  
7 trace metals in atmospheric aerosols in the United Kingdom, *Atmos Environ*, 35, 4581-  
8 4591, 2001.
- 9 Belis, C. A., Karagulian, F., Larsen, B. R., and Hopke, P. K.: Critical review and meta-analysis of  
10 ambient particulate matter source apportionment using receptor models in Europe, *Atmos*  
11 *Environ*, 69, 94-108, DOI 10.1016/j.atmosenv.2012.11.009, 2013.
- 12 Boman, C., Öhman, M., and Nordin, A.: Trace Element Enrichment and Behavior in Wood Pellet  
13 Production and Combustion Processes, *Energ Fuel*, 20, 993-1000, 10.1021/ef050375b,  
14 2006.
- 15 Bruggemann, E., Gnauk, T., Mertes, S., Acker, K., Auel, R., Wieprecht, W., Moller, D., Collett,  
16 J. L., Chang, H., Galgon, D., Chemnitzer, R., Rud, C., Junek, R., Wiedensohler, W., and  
17 Herrmann, H.: Schmucke hill cap cloud and valley stations aerosol characterisation during  
18 FEBUKO (I): Particle size distribution, mass, and main components, *Atmos Environ*, 39,  
19 4291-4303, DOI 10.1016/j.atmosenv.2005.02.013, 2005.
- 20 Burkhard, E. G., Mehmood, G., and Husain, L.: Determination of Trace-Elements in Cloud Water  
21 and Aerosols Using Instrumental Neutron-Activation Analysis and Hydride Generation  
22 with Atomic-Absorption Spectrometry, *J Radioan Nucl Ch Ar*, 161, 101-112, Doi  
23 10.1007/Bf02034884, 1992.
- 24 Cini, R., Prodi, F., Santachiara, G., Porcu, F., Bellandi, S., Stortini, A. M., Oppo, C., Udisti, R.,  
25 and Pantani, F.: Chemical characterization of cloud episodes at a ridge site in Tuscan  
26 Appennines, Italy, *Atmos Res*, 61, 311-334, Pii S0169-8095(01)00139-9, Doi  
27 10.1016/S0169-8095(01)00139-9, 2002.
- 28 Clarke, A. G., and Radojevic, M.: Oxidation of So<sub>2</sub> in Rainwater and Its Role in Acid-Rain  
29 Chemistry, *Atmos Environ*, 21, 1115-1123, Doi 10.1016/0004-6981(87)90238-1, 1987.
- 30 Deguillaume, A. M., Marie, O., Carde, A., Mourey, F., Rouveau, M., Faure, P., Schlemmer, B.,  
31 and Touratier, S.: Long-term evaluation of practices in surgical antibiotic prophylaxis at  
32 Saint Louis Hospital, *Int J Antimicrob Ag*, 24, S226-S226, 2004.
- 33 Deguillaume, L., Leriche, M., Desboeufs, K., Mailhot, G., George, C., and Chaumerliac, N.:  
34 Transition metals in atmospheric liquid phases: Sources, reactivity, and sensitive  
35 parameters, *Chem Rev*, 105, 3388-3431, Doi 10.1021/Cr040649c, 2005.
- 36 Demoz, B. B., Collett, J. L., and Daube, B. C.: On the Caltech Active Strand Cloudwater  
37 Collectors, *Atmos Res*, 41, 47-62, Doi 10.1016/0169-8095(95)00044-5, 1996.
- 38 Dongarra, G., Manno, E., Varrica, D., Lombardo, M., and Vultaggio, M.: Study on ambient  
39 concentrations of PM<sub>10</sub>, PM<sub>10-2.5</sub>, PM<sub>2.5</sub> and gaseous pollutants. Trace elements and  
40 chemical speciation of atmospheric particulates, *Atmos Environ*, 44, 5244-5257, DOI  
41 10.1016/j.atmosenv.2010.08.041, 2010.
- 42 Fine, P. M., Cass, G. R., and Simoneit, B. R. T.: Chemical characterization of fine particle  
43 emissions from fireplace combustion of woods grown in the northeastern United States,  
44 *Environ Sci Technol*, 35, 2665-2675, Doi 10.1021/Es001466k, 2001.

1 Fine, P. M., Cass, G. R., and Simoneit, B. R. T.: Chemical characterization of fine particle  
2 emissions from the wood stove combustion of prevalent United States tree species,  
3 *Environ Eng Sci*, 21, 705-721, DOI 10.1089/ees.2004.21.705, 2004.

4 Fomba, K. W., Muller, K., van Pinxteren, D., and Herrmann, H.: Aerosol size-resolved trace  
5 metal composition in remote northern tropical Atlantic marine environment: case study  
6 Cape Verde islands, *Atmos Chem Phys*, 13, 4801-4814, DOI 10.5194/acp-13-4801-2013,  
7 2013.

8 Guo, J., Wang, Y., Shen, X. H., Wang, Z., Lee, T., Wang, X. F., Li, P. H., Sun, M. H., Collett, J.  
9 L., Wang, W. X., and Wang, T.: Characterization of cloud water chemistry at Mount Tai,  
10 China: Seasonal variation, anthropogenic impact, and cloud processing, *Atmos Environ*,  
11 60, 467-476, DOI 10.1016/j.atmosenv.2012.07.016, 2012.

12 Handler, M., Puls, C., Zbiral, J., Marr, I., Puxbaum, H., and Limbeck, A.: Size and composition  
13 of particulate emissions from motor vehicles in the Kaisermuhlen-Tunnel, Vienna, *Atmos*  
14 *Environ*, 42, 2173-2186, DOI 10.1016/j.atmosenv.2007.11.054, 2008.

15 Harris, E., Sinha, B., van Pinxteren, D., Tilgner, A., Fomba, K. W., Schneider, J., Roth, A.,  
16 Gnauk, T., Fahlbusch, B., Mertes, S., Lee, T., Collett, J., Foley, S., Borrmann, S., Hoppe,  
17 P., and Herrmann, H.: Enhanced Role of Transition Metal Ion Catalysis During In-Cloud  
18 Oxidation of SO<sub>2</sub>, *Science*, 340, 727-730, DOI 10.1126/science.1230911, 2013.

19 Hashimoto, Y., Hwang, J. Y., and Yanagisa, S.: Possible Source of Atmospheric Pollution of  
20 Selenium, *Environ Sci Technol*, 4, 157-162, Doi 10.1021/Es60037a002, 1970.

21 Herckes, P., Engling, G., Kreidenweis, S. M., and Collett, J. L.: Particle size distributions of  
22 organic aerosol constituents during the 2002 Yosemite Aerosol Characterization Study,  
23 *Environ Sci Technol*, 40, 4554-4562, Doi 10.1021/Es0515396, 2006.

24 Herrmann, H., Wolke, R., Muller, K., Bruggemann, E., Gnauk, T., Barzaghi, P., Mertes, S.,  
25 Lehmann, K., Massling, A., Birmili, W., Wiedensohler, A., Wierprecht, W., Acker, K.,  
26 Jaeschke, W., Kramberger, H., Svrčina, B., Bachmann, K., Collett, J. L., Galgon, D.,  
27 Schwirn, K., Nowak, A., van Pinxteren, D., Plewka, A., Chemnitzer, R., Rud, C.,  
28 Hofmann, D., Tilgner, A., Diehl, K., Heinold, B., Hinneburg, D., Knoth, O., Sehili, A. M.,  
29 Simmel, M., Wurzler, S., Majdik, Z., Mauersberger, G., and Muller, F.: FEBUKO and  
30 MODMEP: Field measurements and modelling of aerosol and cloud multiphase  
31 processes, *Atmos Environ*, 39, 4169-4183, DOI 10.1016/j.atmosenv.2005.02.004, 2005.

32 Herrmann, H., Bruggemann, E., Franck, U., Gnauk, T., Loschau, G., Muller, K., Plewka, A., and  
33 Spindler, G.: A source study of PM in Saxony by size-segregated characterisation, *J*  
34 *Atmos Chem*, 55, 103-130, DOI 10.1007/s10874-006-9029-7, 2006.

35 Hueglin, C., Gehrig, R., Baltensperger, U., Gysel, M., Monn, C., and Vonmont, H.: Chemical  
36 characterisation of PM<sub>2.5</sub>, PM<sub>10</sub> and coarse particles at urban, near-city and rural sites in  
37 Switzerland, *Atmos Environ*, 39, 637-651, DOI 10.1016/j.atmosenv.2004.10.027, 2005.

38 Hutchings, J. W., Robinson, M. S., McIlwraith, H., Kingston, J. T., and Herckes, P.: The  
39 Chemistry of Intercepted Clouds in Northern Arizona during the North American  
40 Monsoon Season, *Water Air Soil Poll*, 199, 191-202, DOI 10.1007/s11270-008-9871-0,  
41 2009.

42 Iinuma, Y., Bruggemann, E., Gnauk, T., Muller, K., Andreae, M. O., Helas, G., Parmar, R., and  
43 Herrmann, H.: Source characterization of biomass burning particles: The combustion of  
44 selected European conifers, African hardwood, savanna grass, and German and  
45 Indonesian peat, *J Geophys Res-Atmos*, 112, -, ArtID08209 Doi 10.1029/2006jd007120,  
46 2007.

- 1 Jacob, D. J., and Hoffmann, M. R.: A Dynamic-Model for the Production of H<sup>+</sup>, NO<sub>3</sub><sup>-</sup>, and SO<sub>4</sub><sup>2-</sup>  
2 in Urban Fog, *J Geophys Res-Oc Atm*, 88, 6611-6621, Doi 10.1029/Jc088ic11p06611,  
3 1983.
- 4 Kotronarou, A., and Sigg, L.: SO<sub>2</sub> Oxidation in Atmospheric Water - Role of Fe(II) and Effect  
5 of Ligands, *Environ Sci Technol*, 27, 2725-2735, Doi 10.1021/Es00049a011, 1993.
- 6 Lee, R. E., and Vonlehmd.Dj: Trace Metal Pollution in Environment, *Japca J Air Waste Ma*, 23,  
7 853-857, 1973.
- 8 Li, W. J., Wang, Y., Collett, J. L., Chen, J. M., Zhang, X. Y., Wang, Z. F., and Wang, W. X.:  
9 Microscopic Evaluation of Trace Metals in Cloud Droplets in an Acid Precipitation  
10 Region, *Environ Sci Technol*, 47, 4172-4180, Doi 10.1021/Es304779t, 2013.
- 11 Liu, X.-h., Wai, K.-M., Wang, Y., Zhou, J., Li, P.-h., Guo, J., Xu, P.-j., and Wang, W.-x.:  
12 Evaluation of trace elements contamination in cloud/fog water at an elevated mountain  
13 site in Northern China, *Chemosphere*, 88, 531-541,  
14 <http://dx.doi.org/10.1016/j.chemosphere.2012.02.015>, 2012.
- 15 Maenhaut, W., Raes, N., Chi, X. G., Cafmeyer, J., Wang, W., and Salma, I.: Chemical  
16 composition and mass closure for fine and coarse aerosols at a kerbside in Budapest,  
17 Hungary, in spring 2002, *X-Ray Spectrom*, 34, 290-296, Doi 10.1002/Xrs.820, 2005.
- 18 Maenhaut, W., Raes, N., Chi, X. G., Cafmeyer, J., and Wang, W.: Chemical composition and  
19 mass closure for PM<sub>2.5</sub> and PM<sub>10</sub> aerosols at K-pusztá, Hungary, in summer 2006, *X-  
20 Ray Spectrom*, 37, 193-197, Doi 10.1002/Xrs.1062, 2008.
- 21 Maenhaut, W., Nava, S., Lucarelli, F., Wang, W., Chi, X. G., and Kulmala, M.: Chemical  
22 composition, impact from biomass burning, and mass closure for PM<sub>2.5</sub> and PM<sub>10</sub>  
23 aerosols at Hyytiälä, Finland, in summer 2007, *X-Ray Spectrom*, 40, 168-171, Doi  
24 10.1002/Xrs.1302, 2011.
- 25 Mancinelli, V., Decesari, S., Facchini, M. C., Fuzzi, S., and Mangani, F.: Partitioning of metals  
26 between the aqueous phase and suspended insoluble material in fog droplets, *Ann Chim-  
27 Rome*, 95, 275-290, DOI 10.1002/adic.200590033, 2005.
- 28 Marengo, F., Bonasoni, P., Calzolari, F., Ceriani, M., Chiari, M., Cristofanelli, P., D'Alessandro,  
29 A., Fermo, P., Lucarelli, F., Mazzei, F., Nava, S., Piazzalunga, A., Prati, P., Valli, G., and  
30 Vecchi, R.: Characterization of atmospheric aerosols at Monte Cimone, Italy, during  
31 summer 2004: Source apportionment and transport mechanisms, *J Geophys Res-Atmos*,  
32 111, Artn D24202, Doi 10.1029/2006jd007145, 2006.
- 33 Masiol, M., Squizzato, S., Ceccato, D., and Pavoni, B.: The size distribution of chemical  
34 elements of atmospheric aerosol at a semi-rural coastal site in Venice (Italy). The role of  
35 atmospheric circulation, *Chemosphere*, 119, 400-406, DOI  
36 10.1016/j.chemosphere.2014.06.086, 2015.
- 37 Millero, F. J., Gonzalezdávila, M., and Santanacasio, J. M.: Reduction of Fe(II) with Sulfite in  
38 Natural-Waters, *J Geophys Res-Atmos*, 100, 7235-7244, Doi 10.1029/94jd03111, 1995.
- 39 Minguillon, M. C., Querol, X., Alastuey, A., Monfort, E., Mantilla, E., Sanz, M. J., Sanz, F.,  
40 Roig, A., Renau, A., Felis, C., Miro, J. V., and Artinano, B.: PM<sub>10</sub> speciation and  
41 determination of air quality target levels. A case study in a highly industrialized area of  
42 Spain, *Sci Total Environ*, 372, 382-396, DOI 10.1016/j.scitotenv.2006.10.023, 2007.
- 43 Moroni, B., Castellini, S., Crocchianti, S., Piazzalunga, A., Fermo, P., Scardazza, F., and  
44 Cappelletti, D.: Ground-based measurements of long-range transported aerosol at the rural  
45 regional background site of Monte Martano (Central Italy), *Atmos Res*, 155, 26-36, DOI  
46 10.1016/j.atmosres.2014.11.021, 2015.



- 1 Muller, K., Lehmann, S., van Pinxteren, D., Gnauk, T., Niedermeier, N., Wiedensohler, A., and  
2 Herrmann, H.: Particle characterization at the Cape Verde atmospheric observatory during  
3 the 2007 RHaMBLe intensive, *Atmos Chem Phys*, 10, 2709-2721, 2010.
- 4 Oktavia, B., Lim, L. W., and Takeuchi, T.: Simultaneous Determination of Fe(III) and Fe(II) Ions  
5 via Complexation with Salicylic Acid and 1,10-Phenanthroline in Microcolumn Ion  
6 Chromatography, *Anal Sci*, 24, 1487-1492, DOI 10.2116/analsci.24.1487, 2008.
- 7 Pacyna, E. G., Pacyna, J. M., Fudala, J., Strzelecka-Jastrzab, E., Hlawiczka, S., Panasiuk, D.,  
8 Nitter, S., Pregger, T., Pfeiffer, H., and Friedrich, R.: Current and future emissions of  
9 selected heavy metals to the atmosphere from anthropogenic sources in Europe, *Atmos*  
10 *Environ*, 41, 8557-8566, DOI 10.1016/j.atmosenv.2007.07.040, 2007.
- 11 Pacyna, J. M.: Estimation of the Atmospheric Emissions of Trace-Elements from Anthropogenic  
12 Sources in Europe, *Atmos Environ*, 18, 41-50, 1984.
- 13 Pakkanen, T. A., Kerminen, V. M., Loukkola, K., Hillamo, R. E., Aarnio, P., Koskentalo, T., and  
14 Maenhaut, W.: Size distributions of mass and chemical components in street-level and  
15 rooftop PM<sub>1</sub> particles in Helsinki, *Atmos Environ*, 37, 1673-1690, Doi 10.1016/S1352-  
16 2310(03)00011-6, 2003.
- 17 Parazols, M., Marinoni, A., Amato, P., Abida, O., Laj, P., and Mailhot, G.: Speciation and role of  
18 iron in cloud droplets at the puy de Dome station, *J Atmos Chem*, 54, 267-281, DOI  
19 10.1007/s10874-006-9026-x, 2006.
- 20 Plessow, K., Acker, K., Heinrichs, H., and Moller, D.: Time study of trace elements and major  
21 ions during two cloud events at the Mt. Brocken, *Atmos Environ*, 35, 367-378, Doi  
22 10.1016/S1352-2310(00)00134-5, 2001.
- 23 Raja, S., Raghunathan, R., Yu, X. Y., Lee, T. Y., Chen, J., Kommalapati, R. R., Murugesan, K.,  
24 Shen, X., Qingzhong, Y., Valsaraj, K. T., and Collett, J. L.: Fog chemistry in the Texas-  
25 Louisiana Gulf Coast corridor, *Atmos Environ*, 42, 2048-2061, DOI  
26 10.1016/j.atmosenv.2007.12.004, 2008.
- 27 Rao, X., and Collett, J. L.: The drop size-dependence of iron and manganese concentrations in  
28 clouds and fogs: Implications for sulfate production, *J Atmos Chem*, 30, 273-289, Doi  
29 10.1023/A:1006044614291, 1998.
- 30 Rogula-Kozłowska, W., Klejnowski, K., Rogula-Kopiec, P., Osrodka, L., Krajny, E., Blaszczyk,  
31 B., and Mathews, B.: Spatial and seasonal variability of the mass concentration and  
32 chemical composition of PM<sub>2.5</sub> in Poland, *Air Qual Atmos Hlth*, 7, 41-58, DOI  
33 10.1007/s11869-013-0222-y, 2014.
- 34 Rüd, C.: Bestimmung von Metallen in Aerosolpartikeln und Wolkenwasser mittels Atom-  
35 Absorptionsspektrometrie, Diplomarbeit, Universität Leipzig, 2003.
- 36 Saarikoski, S., Timonen, H., Saarnio, K., Aurela, M., Jarvi, L., Keronen, P., Kerminen, V. M.,  
37 and Hillamo, R.: Sources of organic carbon in fine particulate matter in northern  
38 European urban air, *Atmos Chem Phys*, 8, 6281-6295, 2008.
- 39 Schkolnik, G., and Rudich, Y.: Detection and quantification of levoglucosan in atmospheric  
40 aerosols: A review, *Anal Bioanal Chem*, 385, 26-33, DOI 10.1007/s00216-005-0168-5,  
41 2006.
- 42 Schmidl, C., Marr, I. L., Caseiro, A., Kotianová, P., Berner, A., Bauer, H., Kasper-Giebl, A., and  
43 Puxbaum, H.: Chemical characterisation of fine particle emissions from wood stove  
44 combustion of common woods growing in mid-European Alpine regions, *Atmos Environ*,  
45 42, 126-141, <http://dx.doi.org/10.1016/j.atmosenv.2007.09.028>, 2008.
- 46 Schwanz, M., Warneck, P., Preiss, M., and Hoffmann, P.: Chemical speciation of iron in fog  
47 water, *Contr. Atmos. Phys.*, 71-1, 131-143, 1998.

- 1 Sholkovitz, E. R., Sedwick, P. N., Church, T. M., Baker, A. R., and Powell, C. F.: Fractional  
2 solubility of aerosol iron: Synthesis of a global-scale data set, *Geochim Cosmochim Ac*,  
3 89, 173-189, DOI 10.1016/j.gca.2012.04.022, 2012.
- 4 Siefert, R. L., Johansen, A. M., Hoffmann, M. R., and Pehkonen, S. O.: Measurements of trace  
5 metal (Fe, Cu, Mn, Cr) oxidation states in fog and stratus clouds, *J Air Waste Manage*, 48,  
6 128-143, 1998.
- 7 Simoneit, B. R. T., Schauer, J. J., Nolte, C. G., Oros, D. R., Elias, V. O., Fraser, M. P., Rogge, W.  
8 F., and Cass, G. R.: Levoglucosan, a tracer for cellulose in biomass burning and  
9 atmospheric particles, *Atmos Environ*, 33, 173-182, Doi 10.1016/S1352-2310(98)00145-  
10 9, 1999.
- 11 Spindler, G., Gruner, A., Muller, K., Schlimper, S., and Herrmann, H.: Long-term size-segregated  
12 particle (PM10, PM2.5, PM1) characterization study at Melpitz - influence of air mass  
13 inflow, weather conditions and season, *J Atmos Chem*, 70, 165-195, DOI  
14 10.1007/s10874-013-9263-8, 2013.
- 15 Spokes, L. J., Jickells, T. D., and Lim, B.: Solubilization of Aerosol Trace-Metals by Cloud  
16 Processing - a Laboratory Study, *Geochim Cosmochim Ac*, 58, 3281-3287, Doi  
17 10.1016/0016-7037(94)90056-6, 1994.
- 18 Straub, D. J., Hutchings, J. W., and Herckes, P.: Measurements of fog composition at a rural site,  
19 *Atmos Environ*, 47, 195-205, DOI 10.1016/j.atmosenv.2011.11.014, 2012.
- 20 Tilgner, A., Schöne, L., Bräuer, P., van Pinxteren, D., Hoffmann, E., Spindler, G., Mertes, S.,  
21 Birmili, W., Otto, R., Merkel, M., Weinhold, K., Wiedensohler, A., Deneke, H., Haunold,  
22 W., Engel, A., Wéber, A., and Herrmann, H.: Critical assessment of meteorological  
23 conditions and airflow connectivity during HCCT-2010, *Atmos. Chem. Phys. Discuss.*,  
24 14, 1861-1917, 10.5194/acpd-14-1861-2014, 2014.
- 25 Trapp, J. M., Millero, F. J., and Prospero, J. M.: Trends in the solubility of iron in dust-dominated  
26 aerosols in the equatorial Atlantic trade winds: Importance of iron speciation and sources,  
27 *Geochem Geophys Geosy*, 11, Artn Q03014, Doi 10.1029/2009gc002651, 2010.
- 28 Vlastelic, I., Suchorski, K., Sellegri, K., Colomb, A., Nauret, F., Bouvier, L., and Piro, J. L.: The  
29 trace metal signature of atmospheric aerosols sampled at a European regional background  
30 site (puy de Dme, France), *J Atmos Chem*, 71, 195-212, DOI 10.1007/s10874-014-9290-  
31 0, 2014.
- 32 Vong, R. J., Baker, B. M., Brechtel, F. J., Collier, R. T., Harris, J. M., Kowalski, A. S.,  
33 McDonald, N. C., and McInnes, L. M.: Ionic and trace element composition of cloud  
34 water collected on the Olympic Peninsula of Washington State, *Atmos Environ*, 31, 1991-  
35 2001, Doi 10.1016/S1352-2310(96)00337-8, 1997.
- 36 Wang, Z., Sorooshian, A., Prabhakar, G., Coggon, M. M., and Jonsson, H. H.: Impact of  
37 emissions from shipping, land, and the ocean on stratocumulus cloud water elemental  
38 composition during the 2011 E-PEACE field campaign, *Atmos Environ*, 89, 570-580,  
39 <http://dx.doi.org/10.1016/j.atmosenv.2014.01.020>, 2014.
- 40 Wedepohl, K. H.: The Composition of the Continental-Crust, *Geochim Cosmochim Ac*, 59,  
41 1217-1232, 1995.
- 42 Weller, C., Horn, S., and Herrmann, H.: Effects of Fe(III)-concentration, speciation, excitation-  
43 wavelength and light intensity on the quantum yield of iron(III)-oxalato complex  
44 photolysis, *J Photoch Photobio A*, 255, 41-49, DOI 10.1016/j.jphotochem.2013.01.014,  
45 2013.
- 46 Wrzesinsky, T., and Klemm, O.: Summertime fog chemistry at a mountainous site in central  
47 Europe, *Atmos Environ*, 34, 1487-1496, Doi 10.1016/S1352-2310(99)00348-9, 2000.

1 Zhang, W., Tong, Y. D., Wang, H. H., Chen, L., Ou, L. B., Wang, X. J., Liu, G. H., and Zhu, Y.:  
2 Emission of Metals from Pelletized and Uncompressed Biomass Fuels Combustion in  
3 Rural Household Stoves in China, *Sci Rep-Uk*, 4, Artn 5611, Doi 10.1038/Srep05611,  
4 2014.  
5 Zuo, Y. G., and Hoigne, J.: Photochemical Decomposition of Oxalic, Glyoxalic and Pyruvic-Acid  
6 Catalyzed by Iron in Atmospheric Waters, *Atmos Environ*, 28, 1231-1239, 1994.

7

8



1

2 **Table 1:** Aerosol trace metal concentration averages  $\pm$  standard deviation and ranges during HCCT at the valley stations and results from the FEBUKO experiment by  
3 Rüd (2003) Ref 1 and other studies. Ref 2: G. Boccadifalco, Italy (Dongarra et al., 2010), Ref 3, 4: Auchencorth, Castlemorton, UK (Allen A.G. et al. 2001), Ref 5  
4 and 6; Payerne and Chaumont., Switzerland (Hueglin C. et al. 2005), Ref 7: Venice, Italy (Masiol et al., 2015) , Ref 8: Puy de Dôme, France (Vlastelic et al., 2014),  
5 Ref: 9 K-Puska, Hungary (Maenhaut et al., 2008), Ref 10: Hyytiälä, Finland (Maenhaut et al., 2011), Ref 11: Diabla Gora, Poland (Rogula-Kozłowska et al., 2014).  
6 Ref 12: Bertiz ,Spain (Aldabe et al., 2011), Ref: 13 Monte Cimone, Italy (Marenco et al., 2006), Ref 14: Monte Martono, Italy (Moroni et al., 2015)

Elements		Ti	V	Cr	Mn	Co	Fe	Ni	Cu	Zn	Se	Pb	As	Rb	Sr	
HCCT-2010	PM3.5	Mean $\pm$ SD	0.9 $\pm$ 0.9	0.18 $\pm$ 0.1	2.7 $\pm$ 4.3	0.4 $\pm$ 0.5	0.02 $\pm$ 0.03	16.5 $\pm$ 21.2	0.38 $\pm$ 0.7	0.7 $\pm$ 0.44	11.1 $\pm$ 7.6	0.57 $\pm$ 0.9	1.3 $\pm$ 0.7	0.28 $\pm$ 0.3	0.04 $\pm$ 0.03	0.43 $\pm$ 0.3
		Range	0.04-3.9	0.03-0.4	0.35-21.9	0.01-2.4	0.01-0.11	0.22-111.6	0.02-2.5	0.10-2.19	1.1-32.1	0.02-3.7	0.25-2.9	0.01-1.21	0.01-0.1	0.02-1.7
Ref1	PM2.5	Mean $\pm$ SD	9.6 $\pm$ 10		1.0 $\pm$ 1.4	1.8 $\pm$ 1.4	0.1 $\pm$ 0.1	97 $\pm$ 60	6.1 $\pm$ 3.3	7.2 $\pm$ 3.1	9.2 $\pm$ 4.7	5.6 $\pm$ 2.0	0.2 $\pm$ 0.1			1. $\pm$ 0.8
		Range	1.9–29		0.1–3.5	0.02–5.0	0.01–0.3	14–218	2.4–12	1.2–13	5.9–16	2.5–10	0.04–0.4			0.03–2.9
Ref 2	TSP	Mean $\pm$ SD			1.5 $\pm$ 1.2			0.8 $\pm$ 1.3	1.1 $\pm$ 1.2	5.2 $\pm$ 1.2		10 $\pm$ 1.9				0.41 $\pm$ 1
Ref 3	TSP	Mean $\pm$ SD			1.7 $\pm$ 2.1	0.06 $\pm$ 1.4	78 $\pm$ 2.5	1.3 $\pm$ 1.8	1.1 $\pm$ 2.2	11 $\pm$ 2	1.1 $\pm$ 1.3	7.9 $\pm$ 2.2				0.71 $\pm$ 1.4
Ref 4	PM10	Mean		0.7	2.8		89	1.2	6		0.16	10	0.53	0.3		
Ref 5	PM2.5	Mean		0.8	0.8		26	1.3	6		0.2	4.7	0.16	0.15		
Ref 6	PM10	Mean		2.6	0.5	4.6	340		17	18		8.2				
		Range		1.2-4.8	10-28	0.7-7		102-1152		6-58	6.2-41	<14	2.8-23	<2.3		
Ref 7	PM1	Mean	3.1	3.1	5.9	6.8	66.5	3	3.8	38.8						
	1 to 4	Mean	9.2	0.2	3.2	3.1	53.7	12.6	27.2	49.8						
	PM>4	Mean	8.3		10.1	0.7	12.7	1.1	1.3	3.2						
Ref 8	PM 10	Mean $\pm$ SD	6 $\pm$ 10	0.2 $\pm$ 0.3	1.6 $\pm$ 4.7	2.3 $\pm$ 3.8	0.05 $\pm$ 0.08	62 $\pm$ 89	1.9 $\pm$ 4.2	5.8 $\pm$ 22.1	9.4 $\pm$ 15.2	0.02 $\pm$ 0.03	1.3 $\pm$ 4.4	0.05 $\pm$ 0.06	0.16 $\pm$ 0.23	0.55 $\pm$ 0.79
Ref 9	PM10	Median	4.4			2.6	86		1.93	10		4				
		IQR	3.2-6.0			2.1-4.0	59-137		1.58-3.2	8-18.3		3.2-6.0				
Ref 10	PM2.5	Median	0.92			0.52	17.1	0.5	0.34	6		1.59				
	PM10	Median	5.7			2	67	0.44	0.67	6.7		1.45				
		IQR	2.4-8.4			1.2-2.9	46-98	0.28-0.6	0.38-1.0	2.8-10.3		0.65-3.0				
Ref 11	PM2.5	Mean range						0.4-1.1				2.3-13.7	0.2-0.6			
Ref 12	PM10	Mean	11.26		1.3	2.2	0.12	0.09	0.9	2.03	17.3	0.27	2.88	0.1	0.58	1.2
		Range	3.9-80.9		< 10.9	< 18.2	<0.01-1.1	<0.01-0.7	0.01-21.8	< 8.1	3.0-79.5	0.1-0.6	< 11.6	<0.01-0.7	0.16-2.1	<0.01-5.1
Ref 13	PM10	Mean $\pm$ SD	30 $\pm$ 50	3.1 $\pm$ 1.5		6.2 $\pm$ 7	260 $\pm$ 440	1.4 $\pm$ 0.5	2.9 $\pm$ 3.1	9.9 $\pm$ 6		3.9 $\pm$ 2.4				2.7 $\pm$ 2.8
Ref 14	PM2.5	Mean $\pm$ SD	2.0 $\pm$ 1.6		1.8 $\pm$ 0.85	0.7 $\pm$ 0.5	48 $\pm$ 44	0.5 $\pm$ 0.18	5.0 $\pm$ 1.0	5.9 $\pm$ 3.3		1.7 $\pm$ 0.27				

7 IQR=Inter quartile ranges, All concentrations are in ng/m<sup>3</sup>.

1  
2  
3  
4  
5  
6  
7  
8  
9  
10  
11  
12  
13  
14  
15  
16

Table 2: Correlation coefficients ( $r^2$ ) between levoglucosan and Zn, K, Pb, Fe, and As before (GL) and after (GB) air mass parcel passed through the cloud with p-values less than 5%.

<b>PM<sub>1,2</sub></b>		<b>Zn</b>	<b>K</b>	<b>Pb</b>	<b>AS</b>	<b>Fe</b>	<b>Mn</b>
Levoglucosan	GL	0.59	0.81	0.64	0.97	0.95	0.70
	GB	0.88	0.64	0.54	0.38	0.55	0.66

1 Table 3: Mean and range of trace metal concentrations in cloud water at Mt. Schmücke during HCCT 2010.

	HCCT		[ng/m <sup>3</sup> ]		Ref. A		Ref. B		Ref. C		Ref. D		Ref. E		Ref. F	
	Mean	Range	Mean	Range	Mean	Range	Median	Range	Mean	Range	Mean	Mean	Range	Mean	Range	
Ti	9.18	0.1 - 79.1	2.60	0.01 - 24.1			2.3	< 1 - 466								
V	0.71	0.1 - 2.5	0.19	0.03 - 0.5		0 - 26	1.8	0.4 - 15.0			1.3				1.3	0.5 - 1.4
Cr	5.54	0.3 - 52	1.54	0.11 - 14	0.52	< 9.3	< 0.3	< 0.3 - 9.0				1.1		< 3.6		
Mn	5.59	0.1 - 30.1	1.50	0.01 - 8.1		4.8 - 133	7.8	1.0 - 158	66.3	< 1645	1.1				4.4	3.2 - 14.0
Co	0.46	0.1 - 3.5	0.13	0.01 - 0.9			0.08	< 0.02 - 2.1								
Se	1.38	0.1 - 4.9	0.42	0.01 - 1.7		< 9.6			13.2	< 99.9		4.7		1.1 - 11.5		
Pb	1.40	0.3 - 10.5	0.38	0.04 - 2	4.2	2.8 - 63	11	1.97 - 84.0			0.5	27.6		3.4 - 61.4	0.6	0.4 - 2.3
As	0.63	0.2 - 4.1	0.15	0.03 - 0.4			0.4	0.4 - 6.6				3.1		< 13.2		
Rb	0.57	0.1 - 1.7	0.16	0.01 - 0.3			< 1	< 1 - 6								
Sr	2.45	0.2 - 13.5	0.66	0.02 - 3.6			2.3	0.1 - 68.7								

2 Concentrations are in µg/l except otherwise mentioned

Ref. A	Rüd 2003	Mt. Schmücke
Ref. B	Plessow et al.	Mt. Brocken
Ref. C	Guo et al.	Mt. Tai
Ref. D	Vong et al.	Marine clouds
Ref. E	Wrzesinsky and Klemm(2000)	Fichtelgebirge
Ref. F	Straub et al.	Fog in rural Pennsylvania

3

1

2 Table 4: PM<sub>10</sub> soluble aerosol trace metal content at the upwind station Goldlauter (GL), downwind station Gehlberg (GB) and soluble  
 3 trace metals in cloud water at Mt. Schmücke (SM) during four FCE.

EVENTS		Ti	V	Cr	Mn	Fe	Ni	Cu	Zn	As	Se	Rb	Sr	Pb
FCE 1.1	GL	0.27	0.19	0.37	1.01	1.81	0.69	1.77	13.63	0.80	0.32	0.21	0.81	0.95
	SM	0.15	0.17	0.93	<b>0.57</b>	<b>1.69</b>	<b>0.14</b>	<b>1.35</b>		0.08	0.32	0.07	0.89	0.48
	GB	0.09	0.24	0.46	0.84	-	0.39	1.34	13.68	0.62	0.32	0.11	0.72	1.53
FCE11.3	GL	0.40	0.00	0.25	0.19	1.20	0.18	0.37	7.38	0.39	0.17	0.19	0.25	0.26
	SM	0.11	0.00	0.24	0.38					0.02	0.51	0.11	0.35	0.34
	GB	0.28	0.00	0.47	0.34	0.64	0.22	-	9.86	0.60	0.71	0.08	0.74	0.39
FCE13.3	GL	0.10	0.11	0.28	0.70	5.82	0.70	3.23	5.28	0.22	1.09	0.16	0.33	0.88
	SM	0.41	0.16	0.23	0.64					0.08	0.64	0.16	0.40	0.58
	GB	-	0.06	0.45	0.42	3.86	0.24	0.73	4.08	0.19	0.63	0.10	0.16	0.97
FCE22.1	GL	0.12	0.00	1.19	0.30	1.14	0.43	0.54	3.48	0.30	0.12	0.12	0.30	0.36
	SM	0.31	0.10	0.29	0.61					0.10	0.10	0.10	0.61	0.98
	GB	0.38	0.12	0.20	0.16	1.44	0.10	-	2.36	0.08	0.06	0.06	0.22	0.29

4 Concentrations are in ng/m<sup>3</sup>

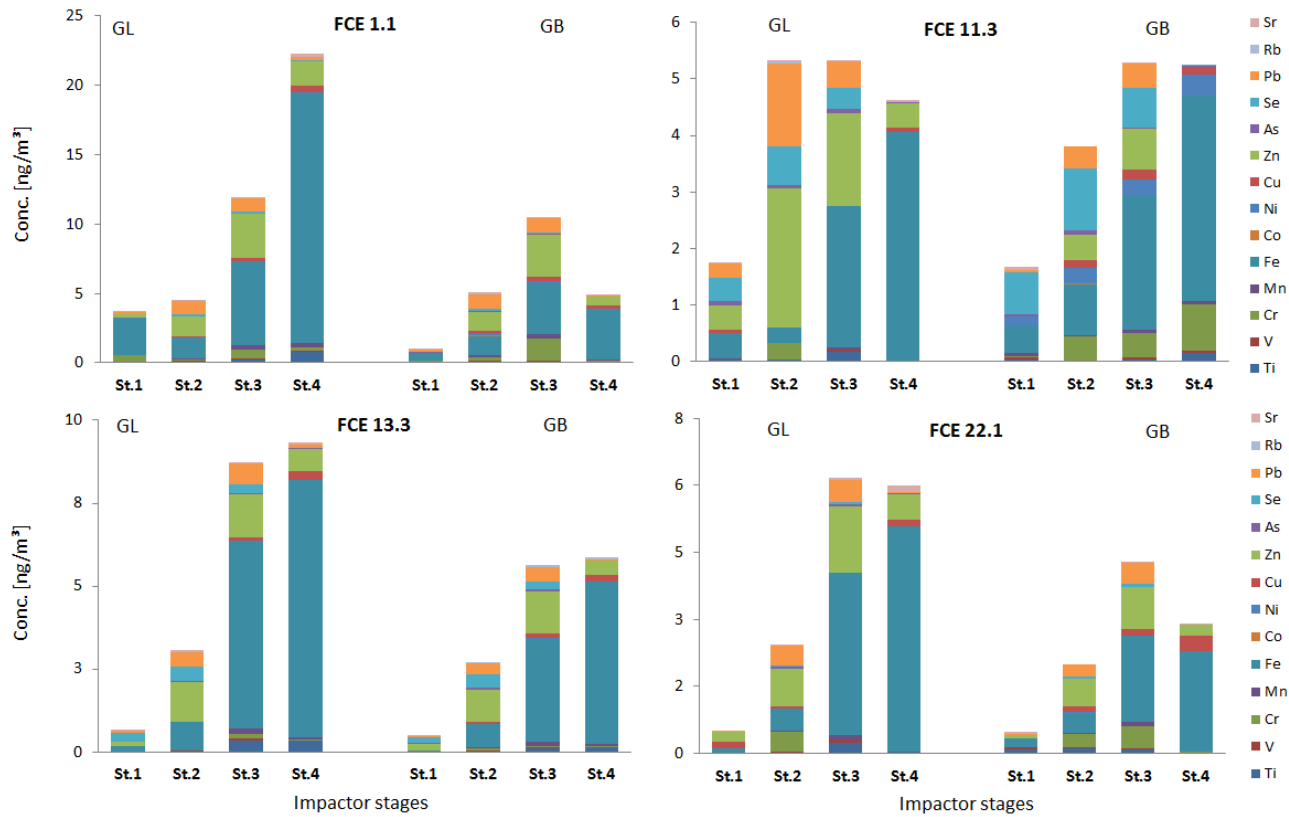
5

6



1

2



3

4

5 Figure 1: Aerosol particle size resolved trace metal concentrations during four full cloud events at Goldlauter (GL) and Gehlberg (GB).

6 The PM stage cut offs for St. 1 to St. 4 are 0.05, 0.14, 0.42, 1.2, and 3.5 $\mu$ m, respectively.

7

8

1  
2  
3  
4  
5  
6  
7  
8  
9  
10  
11  
12

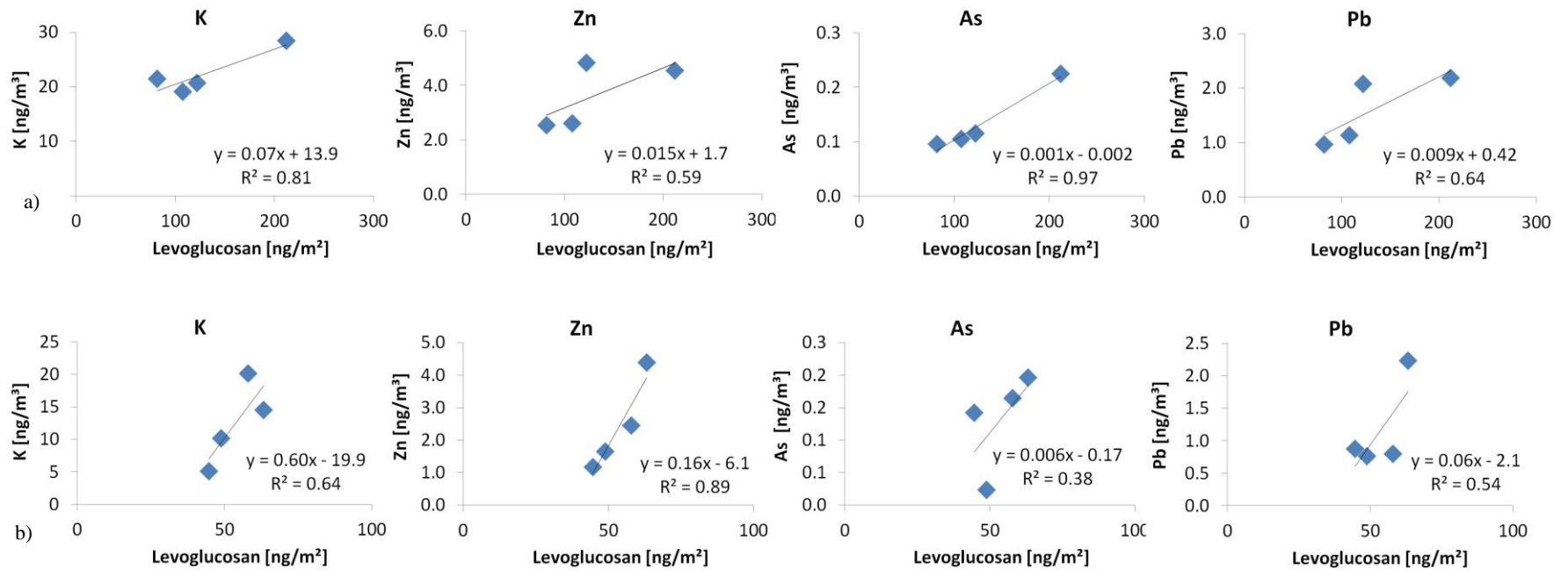
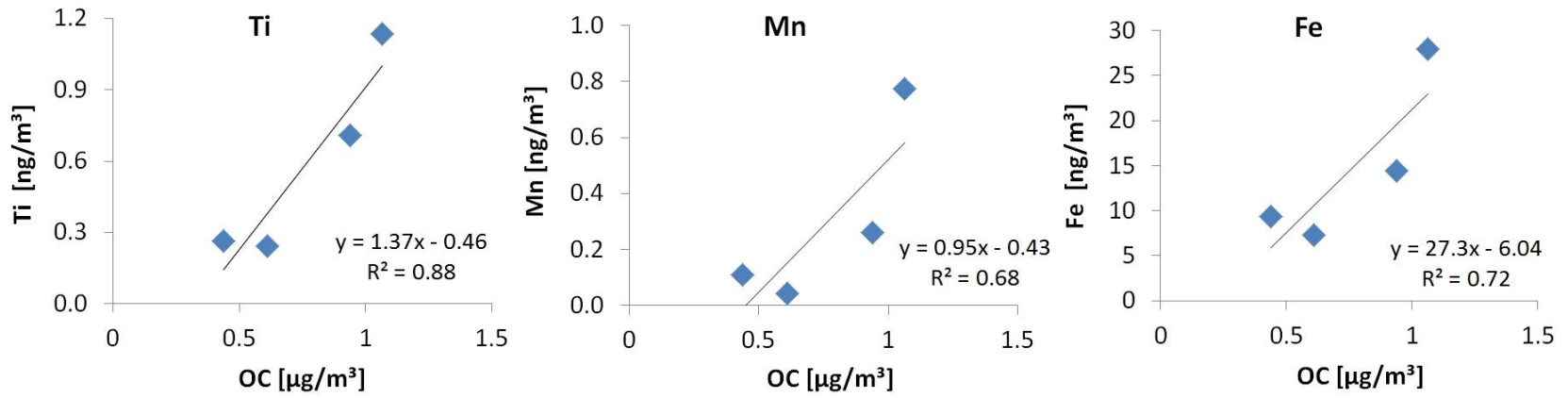


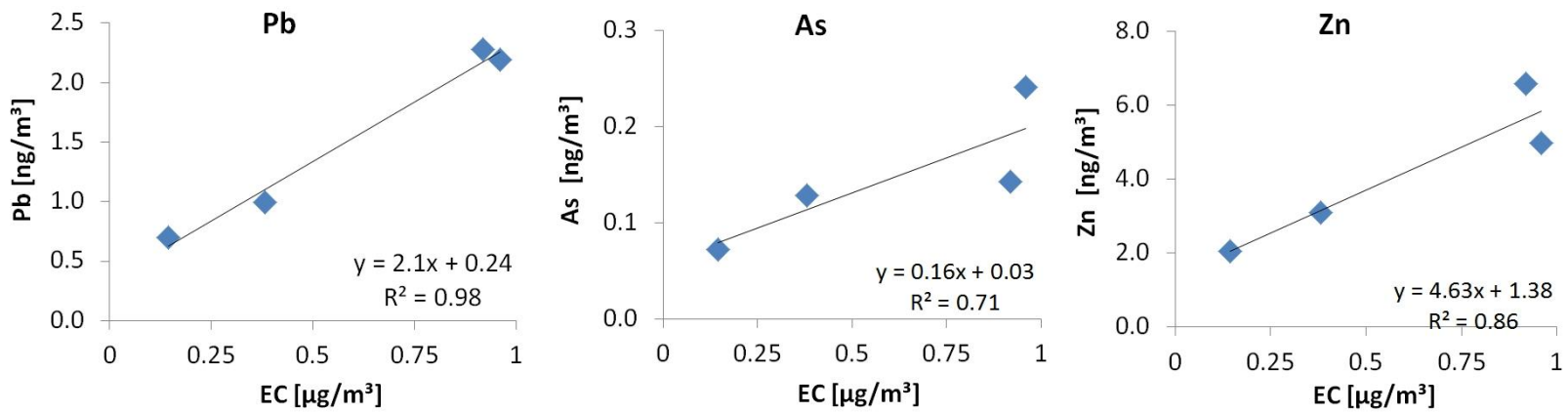
Figure 2: Scatter plots of levoglucosan a biomass burning tracer and K, Zn, As and Pb, in PM<sub>1.2</sub> particulate matter at a) upwind GL and b) downwind GB stations during HCCT2010.

1  
2



3  
4

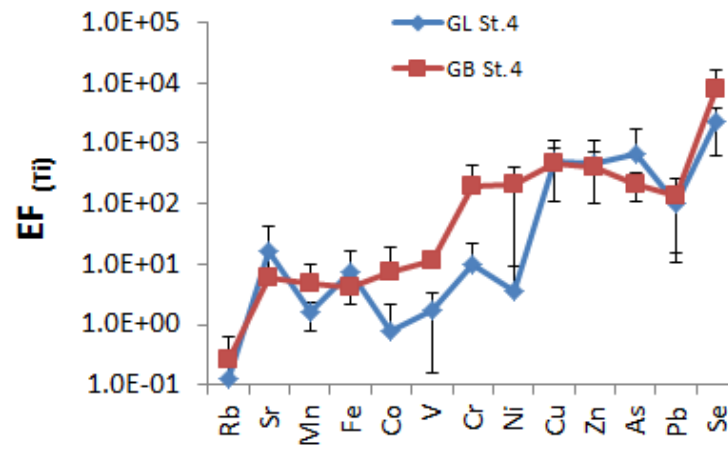
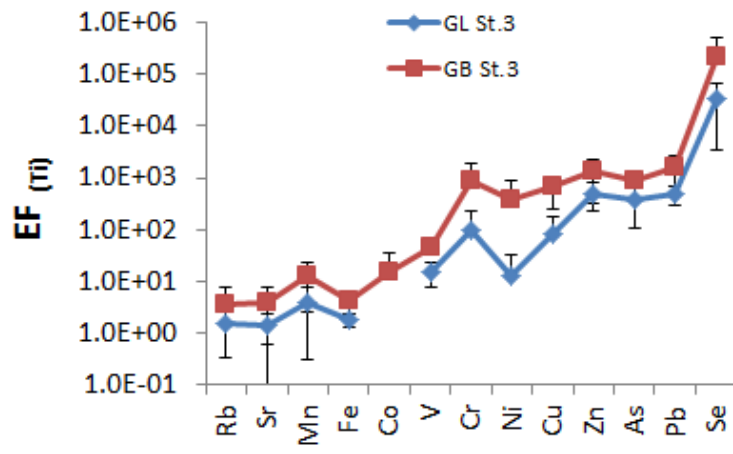
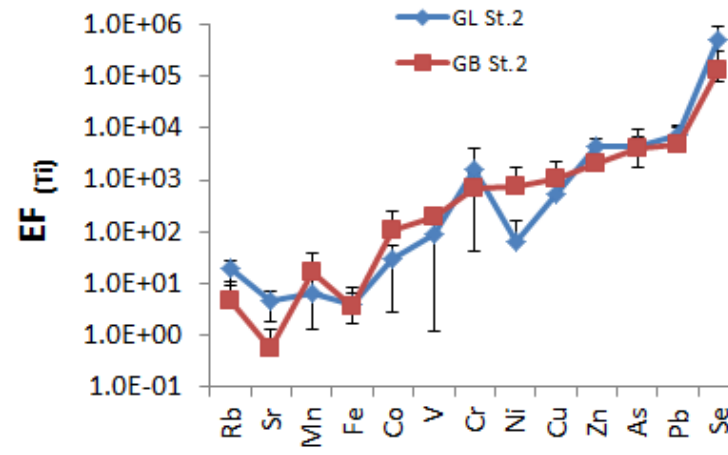
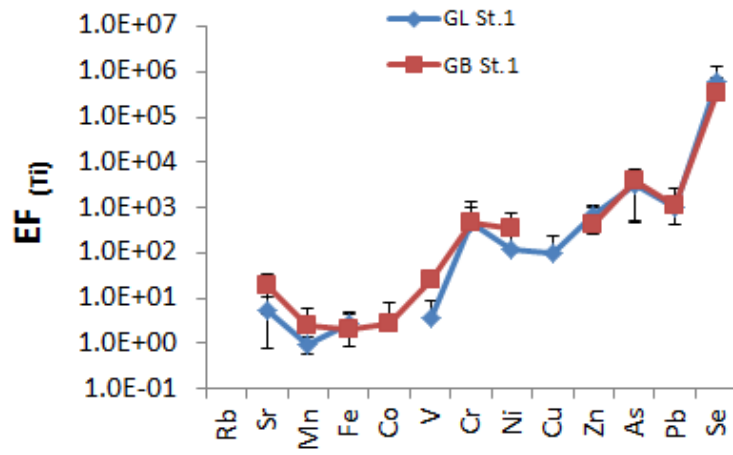
5 Figure 3: PM<sub>3,5</sub> scatter plots of Ti, Mn and Fe against OC at the upwind stations.



6  
7  
8

Figure 4: PM<sub>3,5</sub> scatter plots of Pb, As, Zn against EC at the upwind stations.

1



2

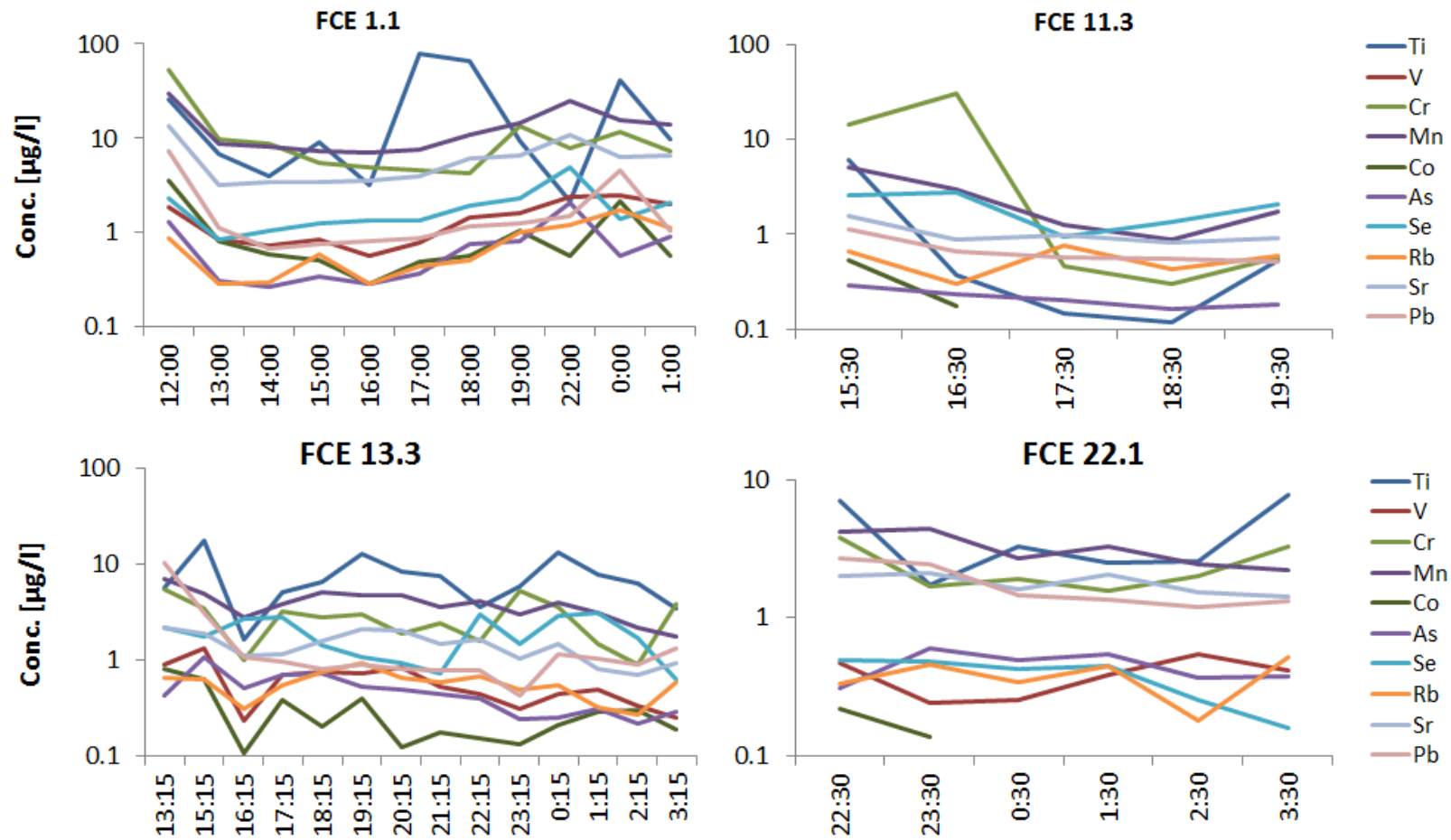
Figure 5: Size resolved enrichment factor analysis of aerosol trace metals at the valley stations. Plotted values are average over all FCE with their respective standard deviations plotted as error bars.

3

4

5

1

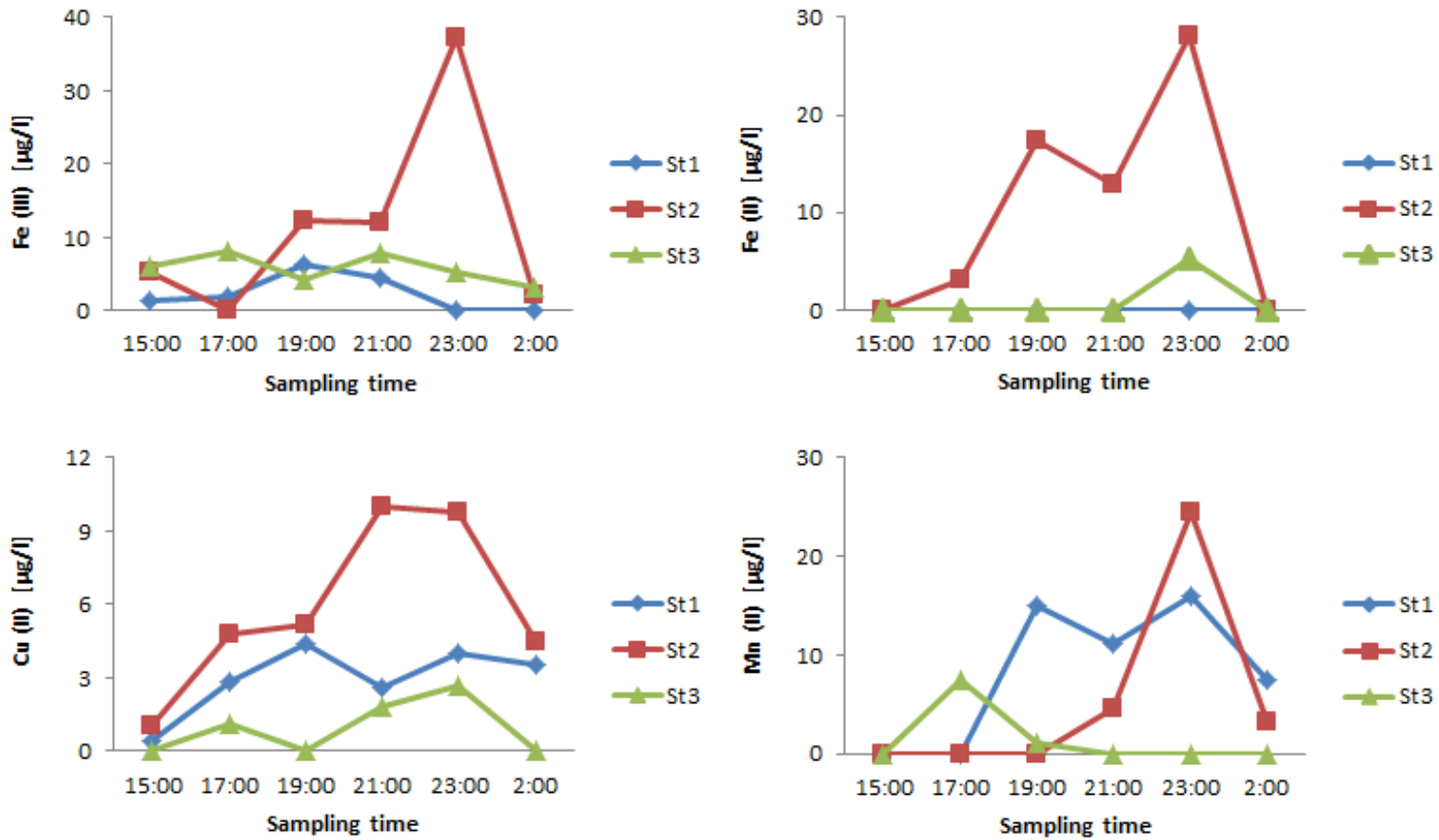


2

3 Figure 6: Trends in total trace metal cloud water concentrations during selected full cloud events, FCE 1.1: 14-15/09/2010, FCE 11.3:  
4 02/10/2010, FCE 13.3: 06-07/10/2010 and FCE 22.1:19-20/10/2010.

5

6



1

2 Figure 7: Temporal variation of size resolved soluble transition metal ions, Fe (III), Fe (II), Cu (II) and Mn (II) in cloud water on the 14-  
 3 15/09/2010 during FCE 1.1. The nominal stage cut-offs were 22 µm, 16 µm and 4 µm for st1, st2 and st3, respectively.

4